



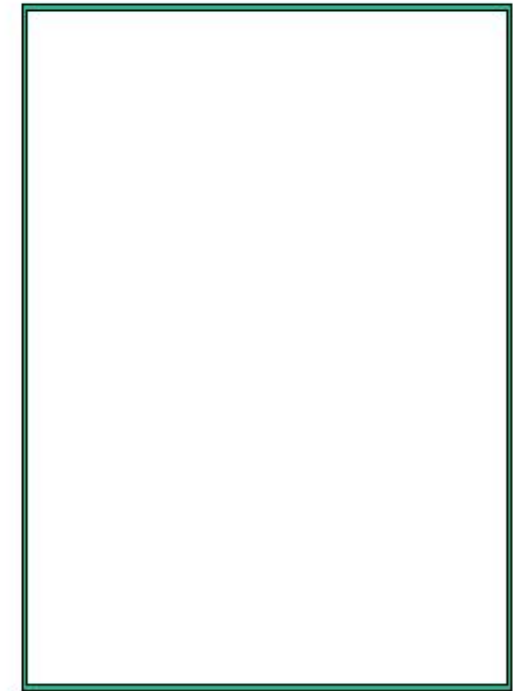
**Hottest**



**Least viscous**



**Most vortical**



???

Supported in part by



U.S. DEPARTMENT OF  
**ENERGY**

## STAR experiment results from Beam Energy Scan program

Alexey Aparin for the STAR collaboration  
Joint Institute for Nuclear Research



Part of this work has been supported by Russian Science Foundation under grant № 22-72-10028



# Beam Energy Scan to map the QCD phase diagram



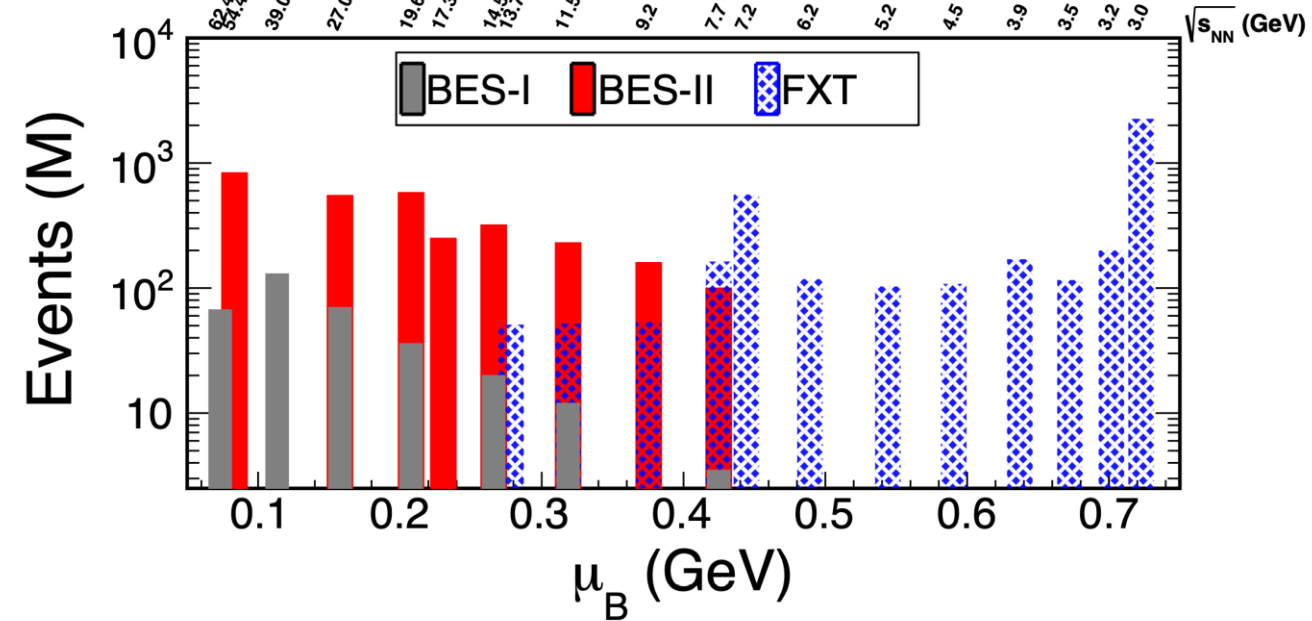
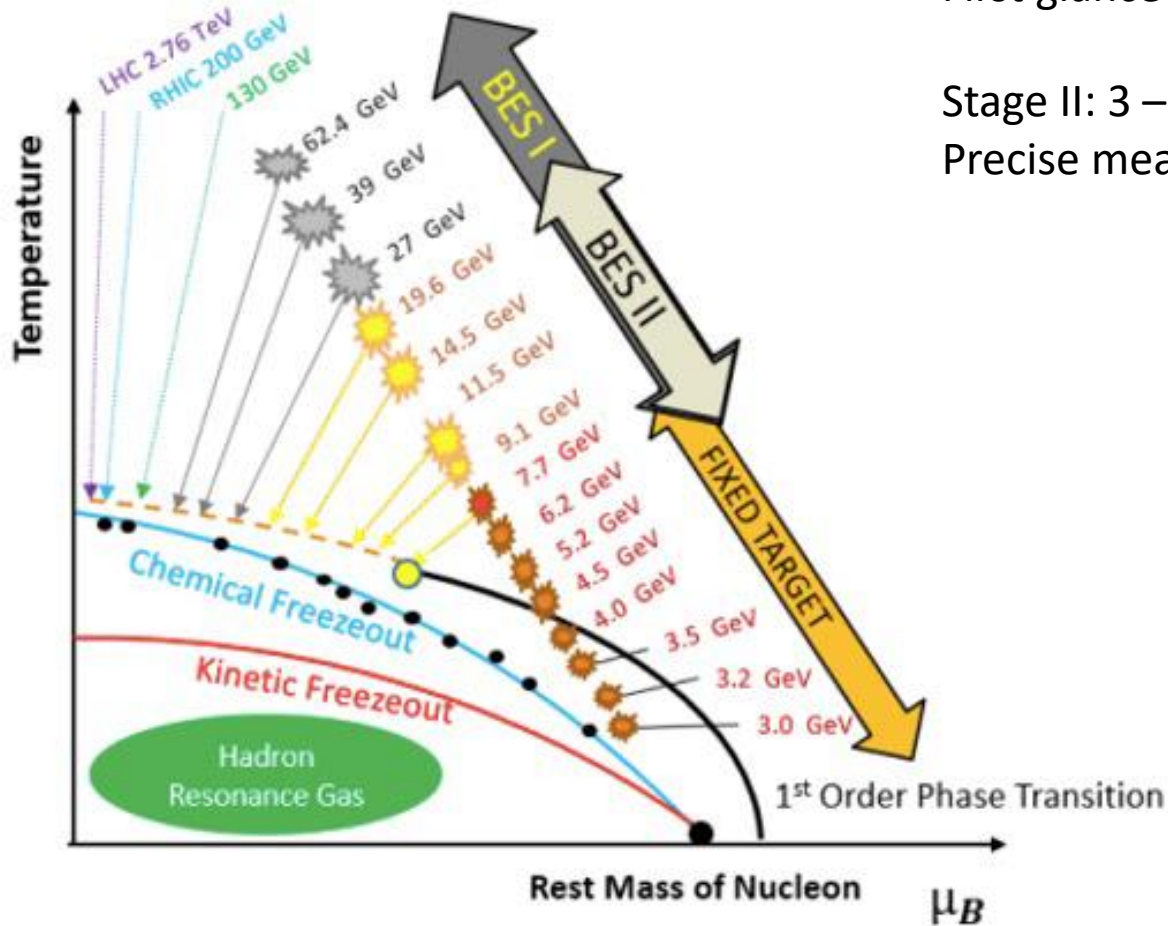
Two stages of Beam Energy Scan:

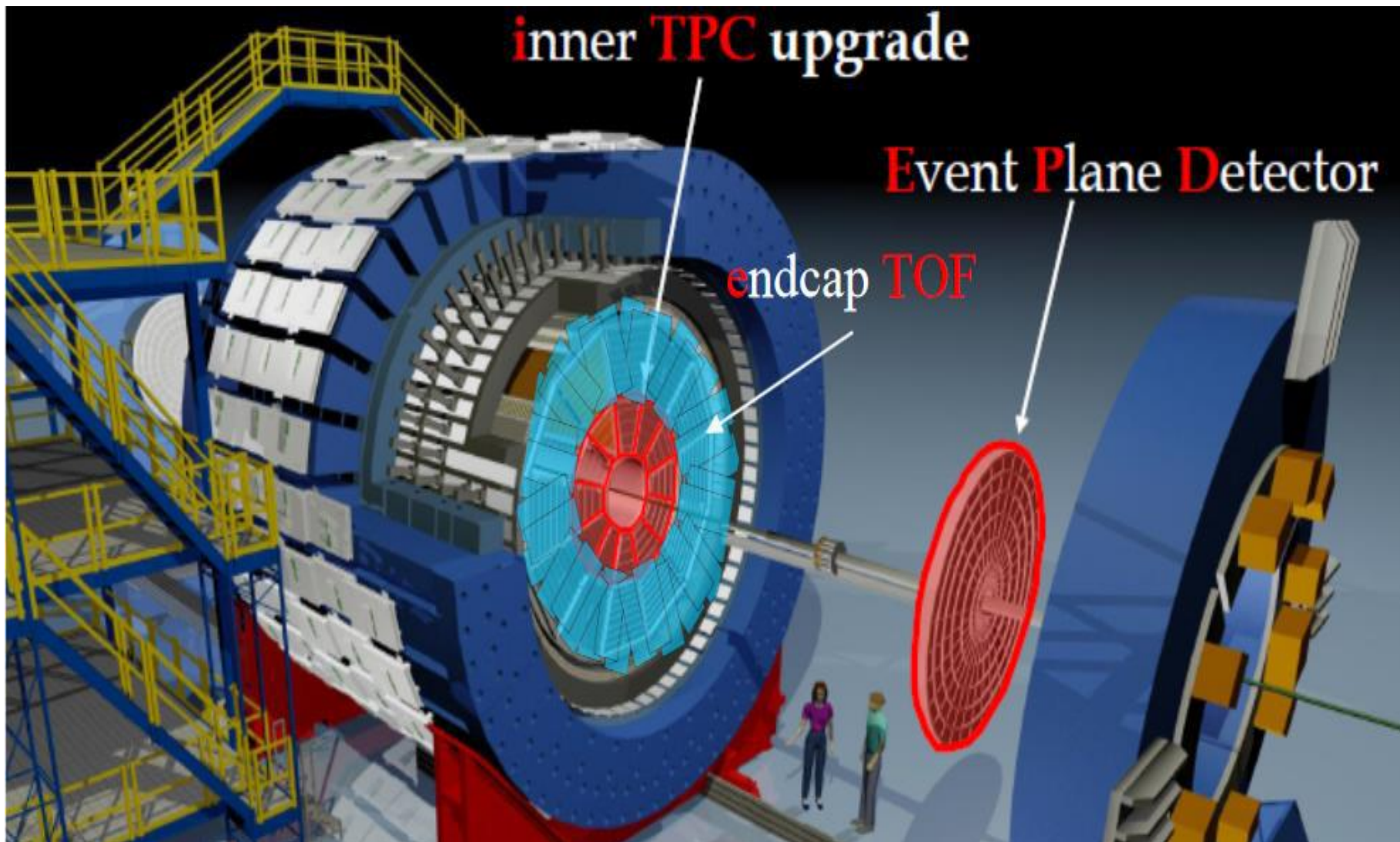
Stage I: 7.7 – 39 GeV 2010 – 2014

First glance at low energy region, rather low statistics

Stage II: 3 – 54.4 GeV 2017 – 2021

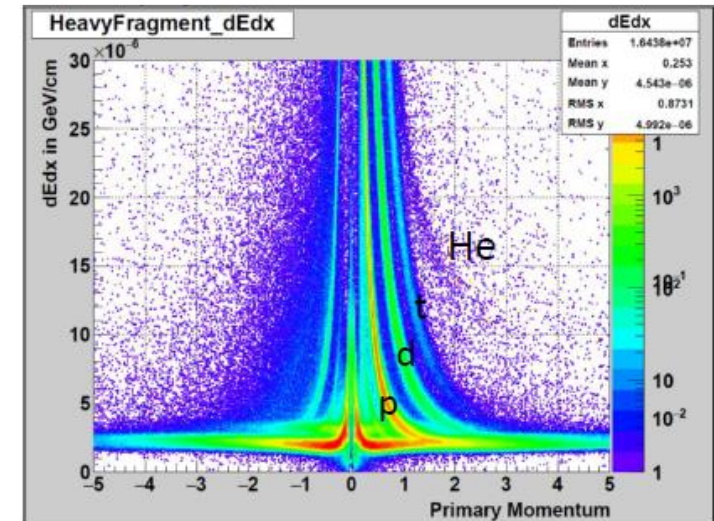
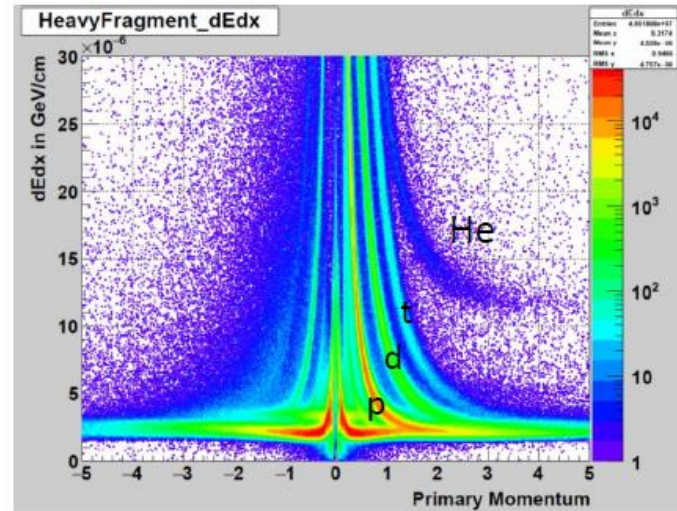
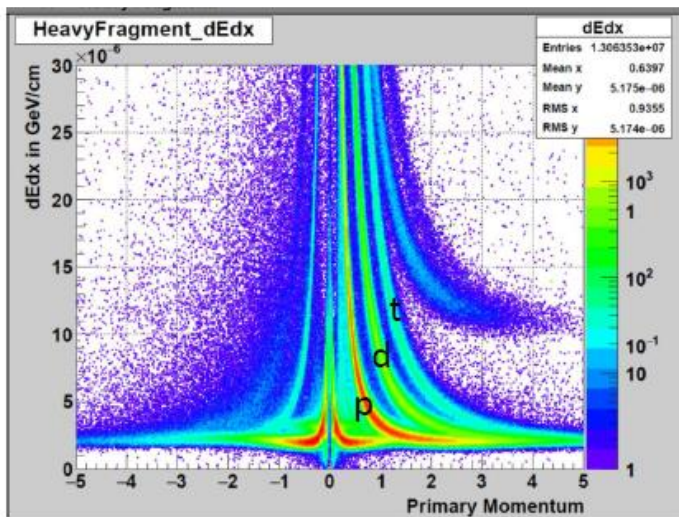
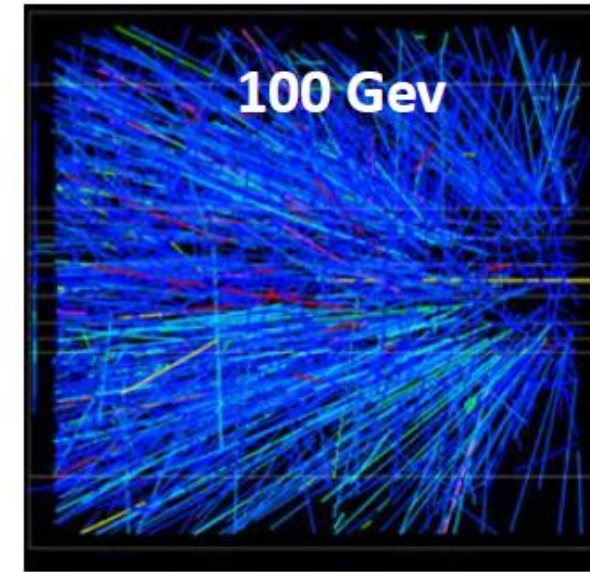
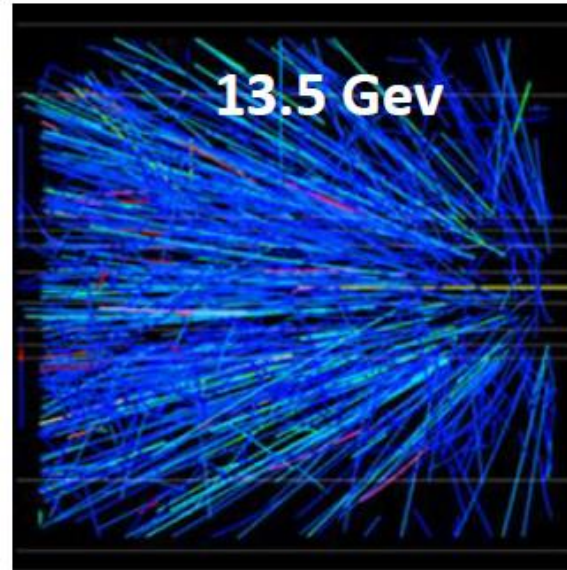
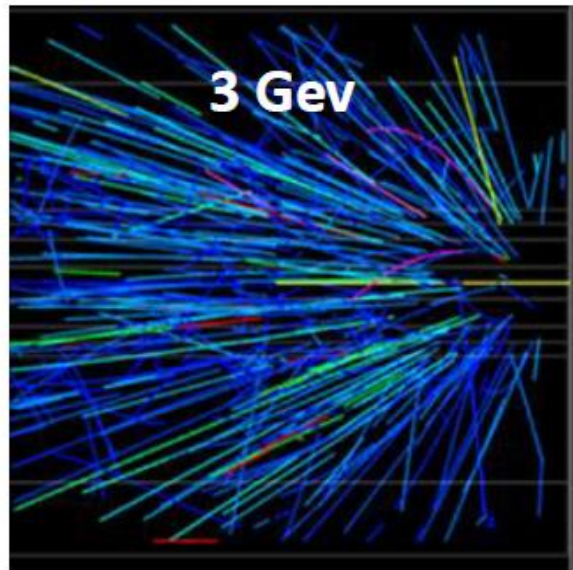
Precise measurements at low energies, large statistics

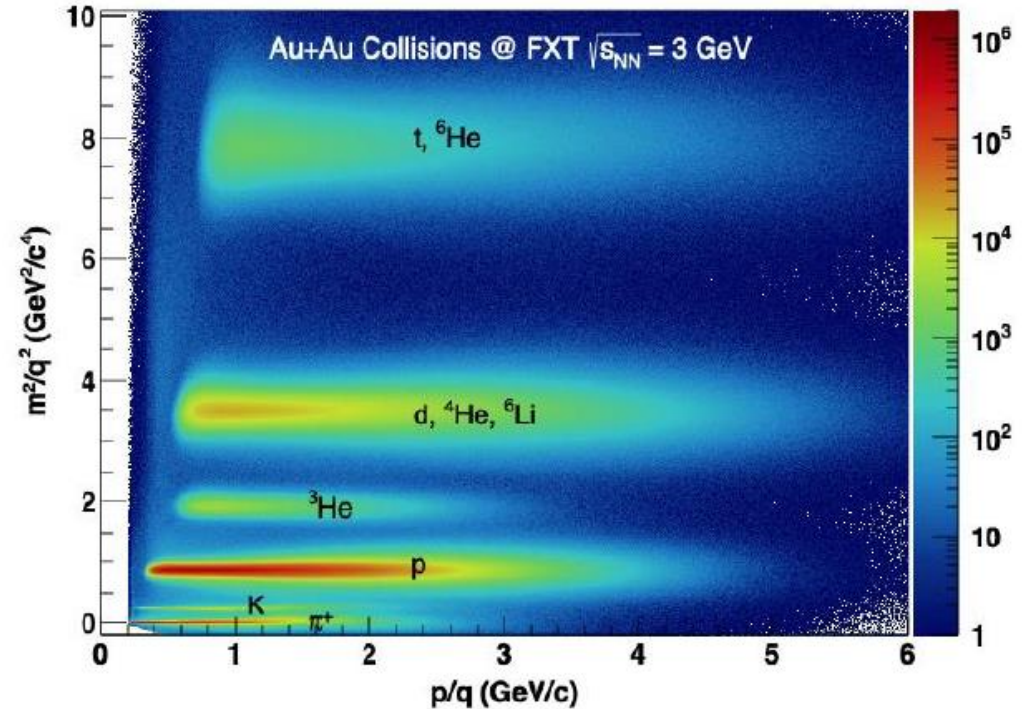
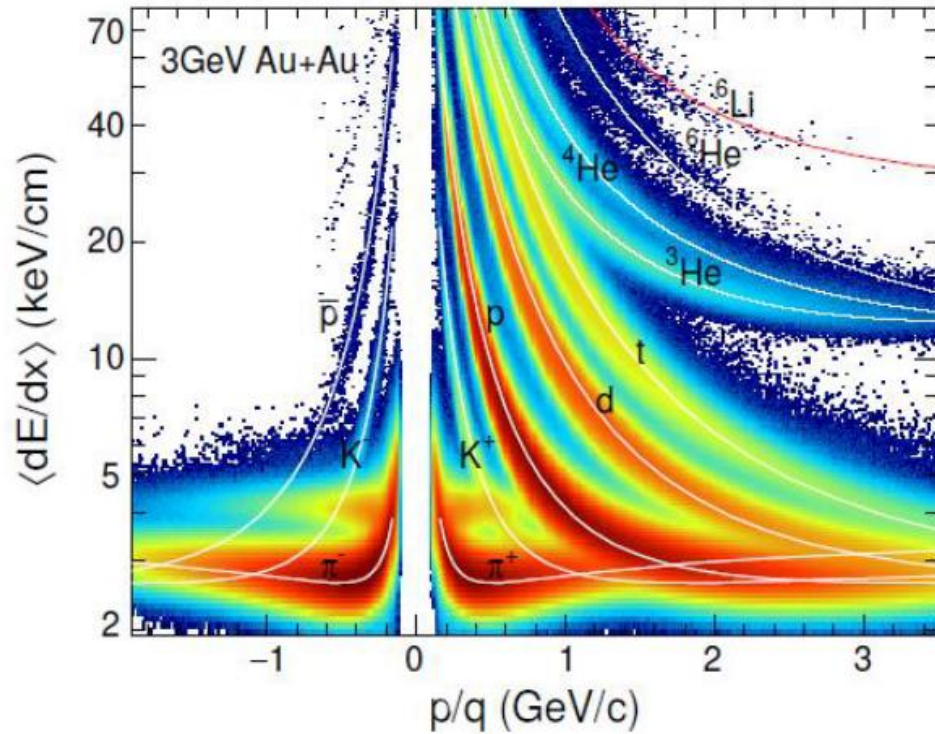
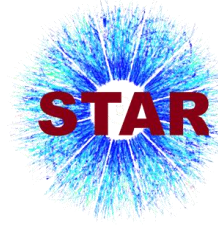




- **Tracking and PID (full  $2\pi$ )**  
TPC:  $|\eta| < 1$   
**iTPC (2019+):  $|\eta| < 1.5$**   
TOF:  $|\eta| < 1$   
**eTOF (2019+):  $-1.6 < \eta < -1$**   
BEMC:  $|\eta| < 1$   
EEMC:  $1 < \eta < 2$   
HFT (2014-2016):  $|\eta| < 1$   
MTD (2014+):  $|\eta| < 0.5$  (partial azimuthal coverage)
- **MB trigger and event plane reconstruction**  
BBC (before 2018):  $3.3 < |\eta| < 5$   
**EPD (2018+):  $2.1 < |\eta| < 5.1$**   
VPD:  $4.2 < |\eta| < 5$   
ZDC:  $6.5 < |\eta| < 7.5$
- **Recent upgrades 2022**  
FCS:  $2.5 < |\eta| < 4$   
FTS:  $2.5 < |\eta| < 4$   
ECAL & HCAL:  $2.5 < |\eta| < 4$

# TPC coverage at FXT energies

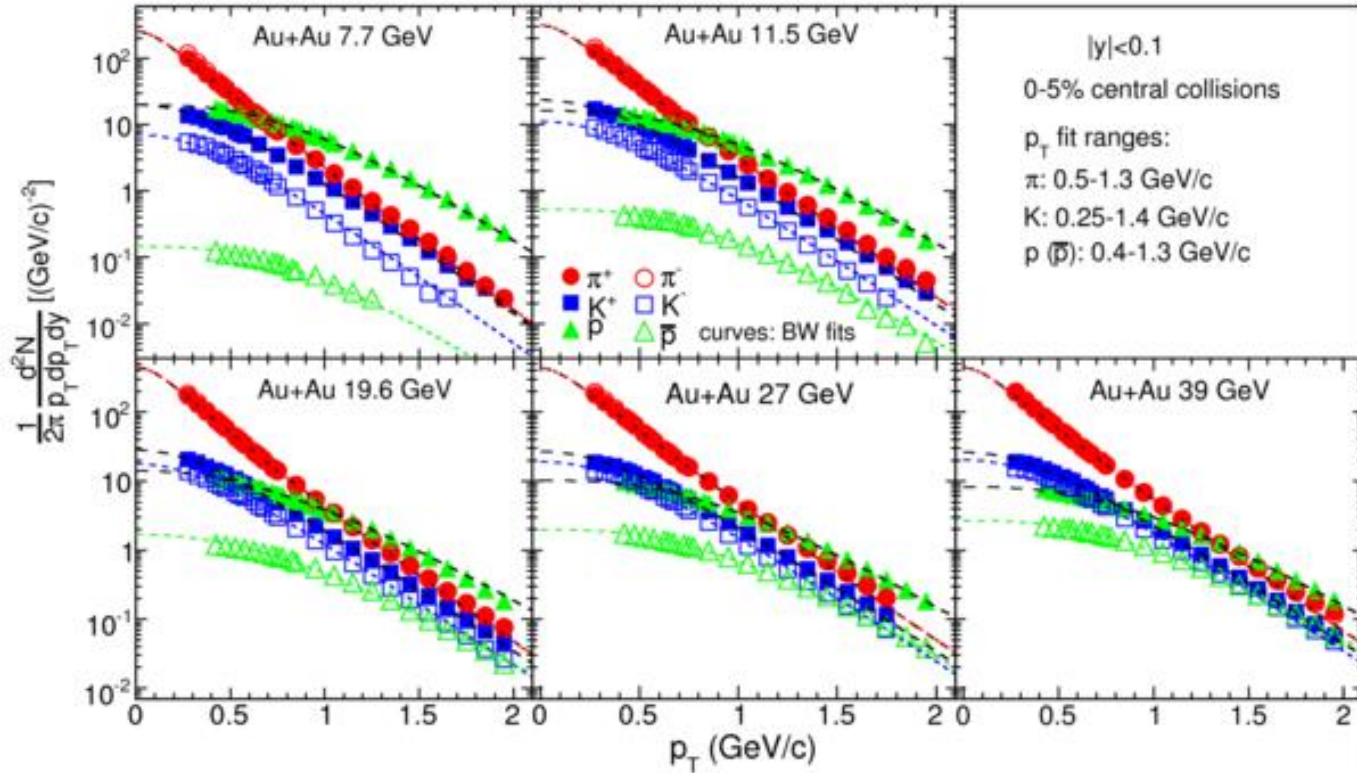




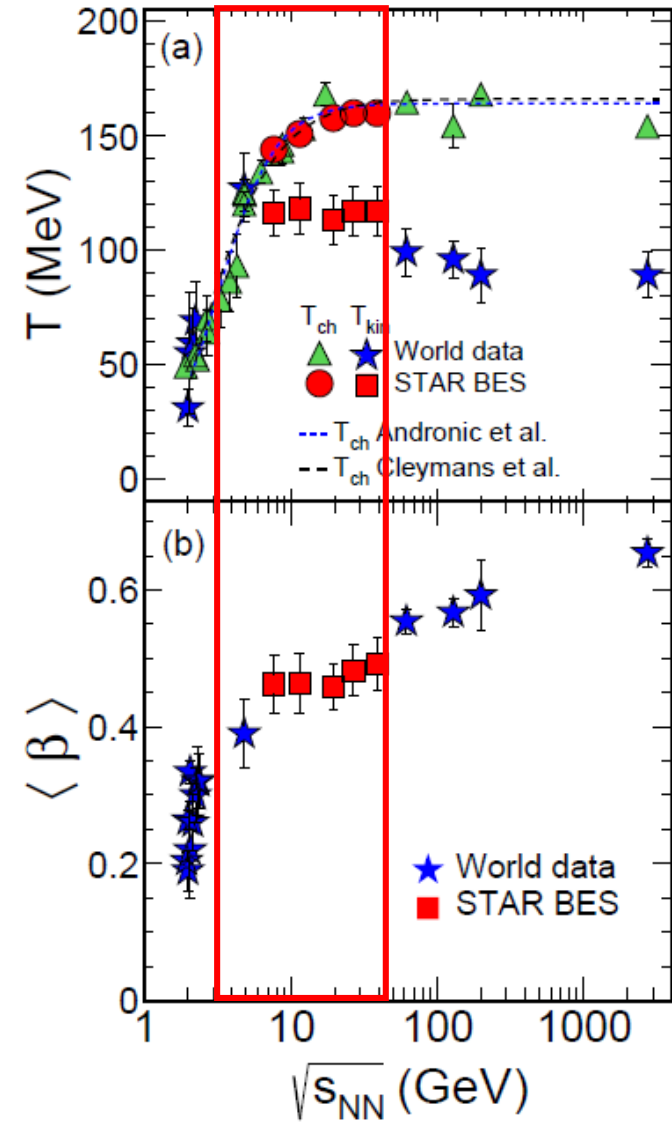
Detects particles in the  $0 < \eta < 2$  range  
 $\pi$ , K, p, d, t, h,  $\alpha$  through dE/dx and ToF  
 $K_s^0$ ,  $\Lambda$ ,  $\Xi$ ,  $\Omega$ ,  $\varphi$ ,  $^3_{\Lambda}\text{H}$ ,  $^4_{\Lambda}\text{H}$  trough invariant mass

About 300M events analyzed from 2018,  
 2B more recorded in 2021

# Collectivity and temperature of the medium



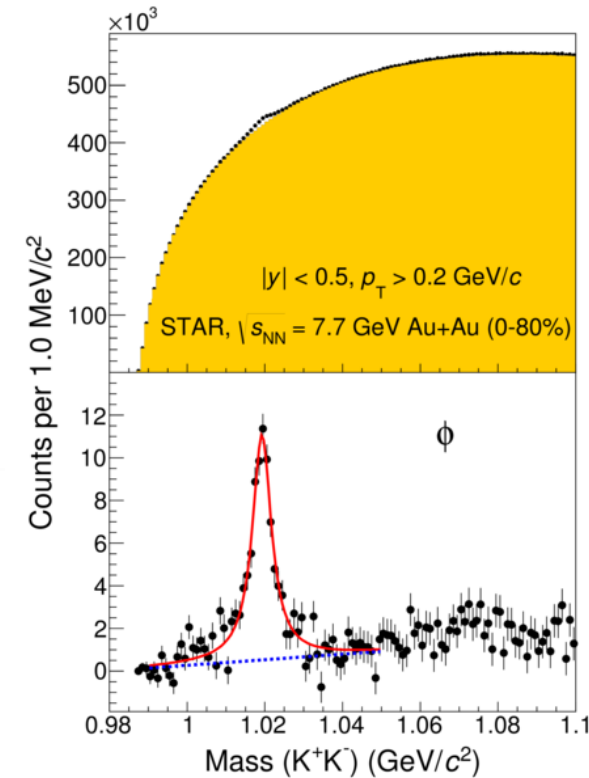
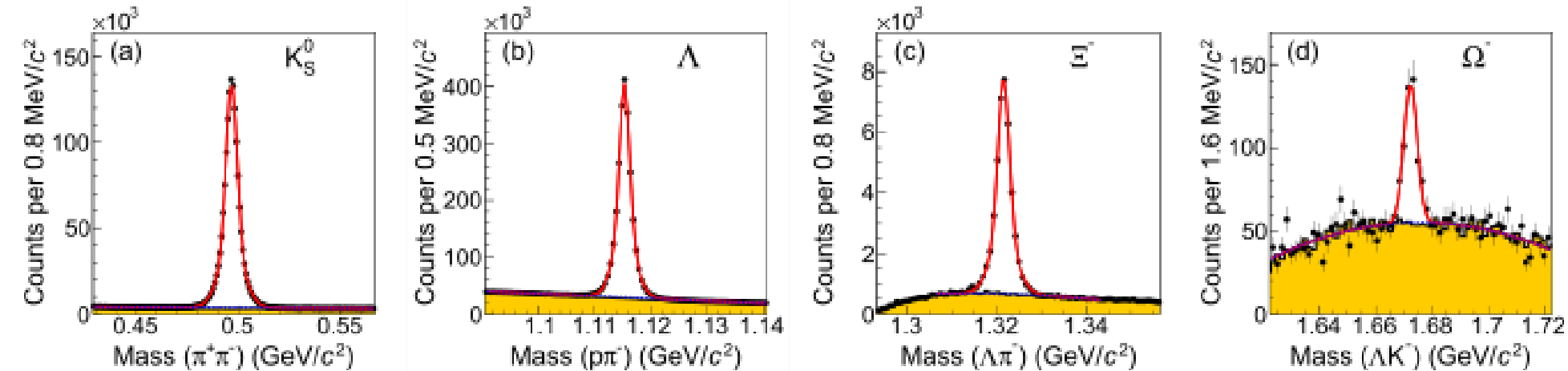
Parameters: Temperature ( $T_{kin}$ ) and transverse radial velocity ( $\beta$ ) obtained by fitting the momentum distribution of particles.



# Strange particle production at BES-I



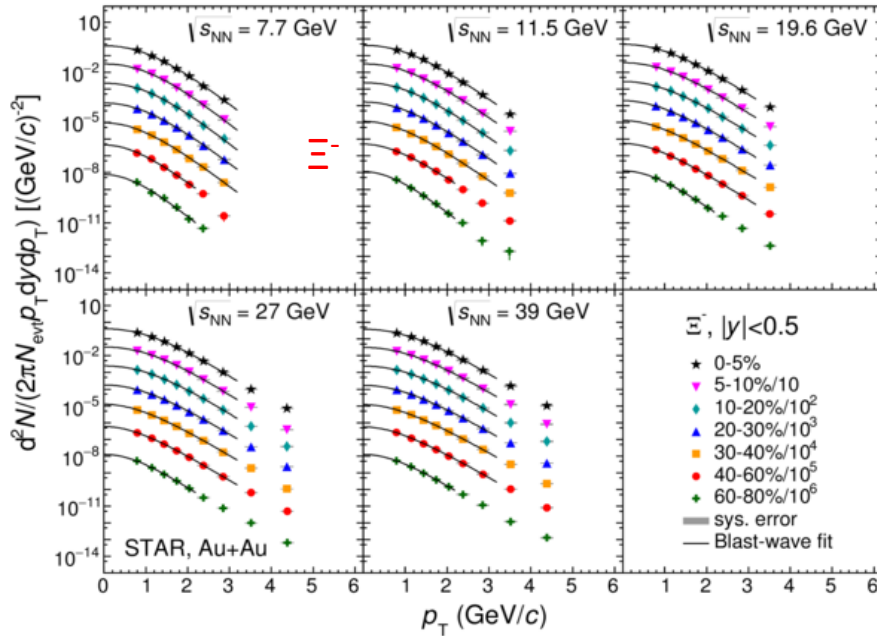
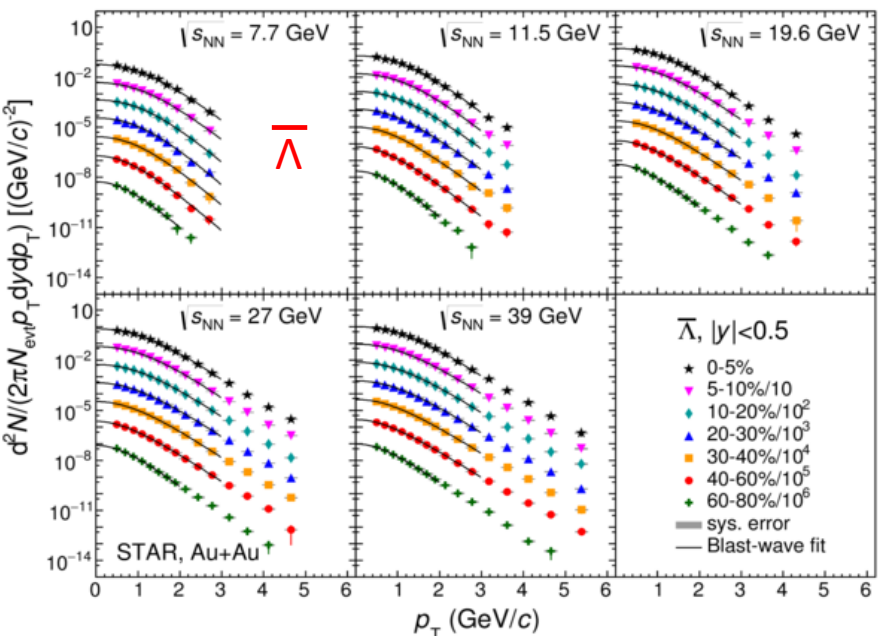
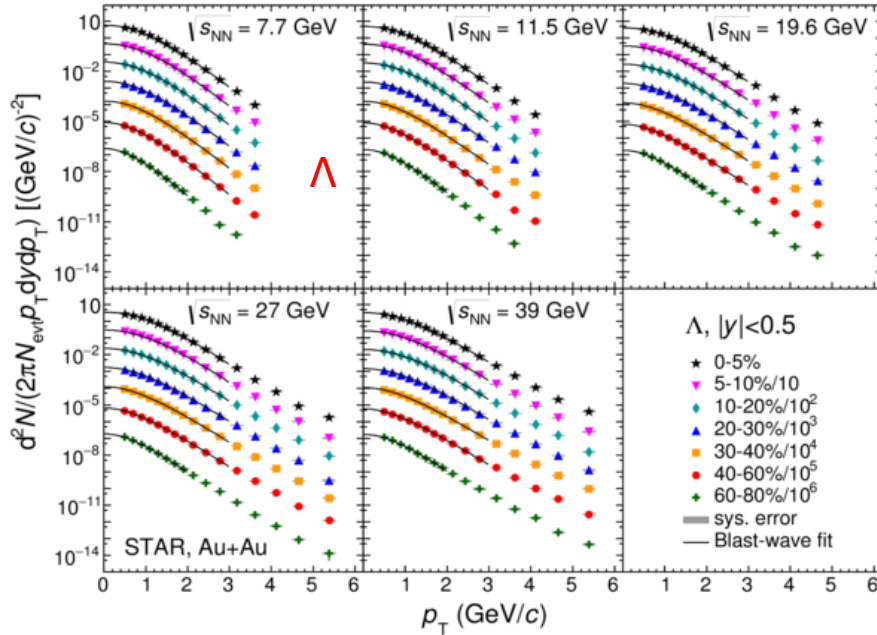
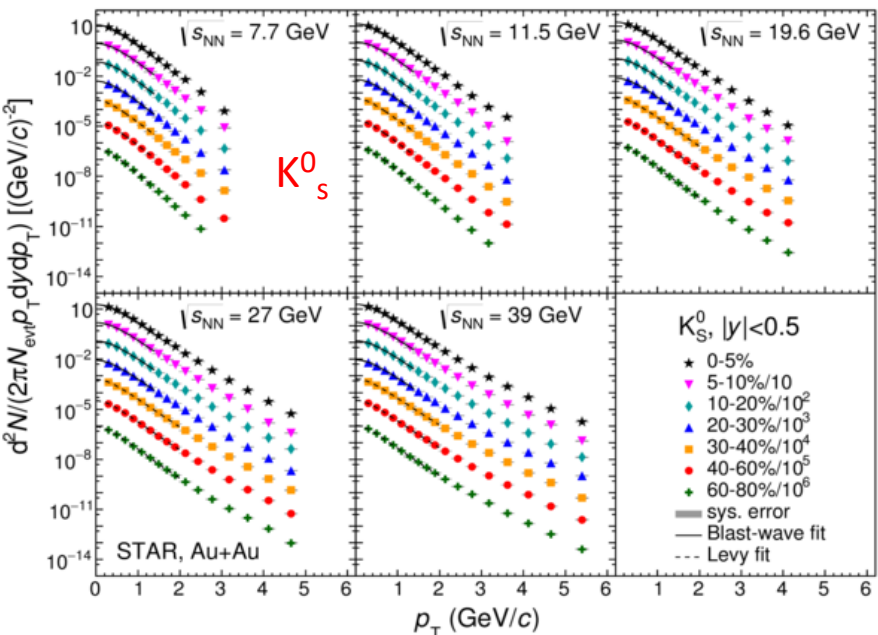
STAR,  $\sqrt{s_{NN}} = 7.7$  GeV Au+Au (0-80%),  $|\eta| < 0.5$



$\sqrt{s_{NN}}$ (GeV)	$z$ -vertex range (cm)	MB events ( $10^6$ )
7.7	[-70, 70]	4.4
11.5	[-50, 50]	12.0
19.6	[-70, 70]	36.3
27	[-70, 70]	72.8
39	[-40, 40]	134.3

$K_S^0 \rightarrow \pi^+ + \pi^-$ , 69.20%;  
 $\Lambda(\bar{\Lambda}) \rightarrow p(\bar{p}) + \pi^-(\pi^+)$ , 63.9%;  
 $\Xi^-(\bar{\Xi}^+) \rightarrow \Lambda(\bar{\Lambda}) + \pi^-(\pi^+)$ , 99.887%;  
 $\Omega^-(\bar{\Omega}^+) \rightarrow \Lambda(\bar{\Lambda}) + K^-(K^+)$ , 67.8%;  
 $\phi \rightarrow K^+ + K^-$ , 49.1%.

# Strange particle production at BES-I



$K_S^0$ ,  $\Lambda$ , anti- $\Lambda$ ,  $E^-$  transverse momentum spectra at midrapidity  $|y| < 0.5$

Levy fit

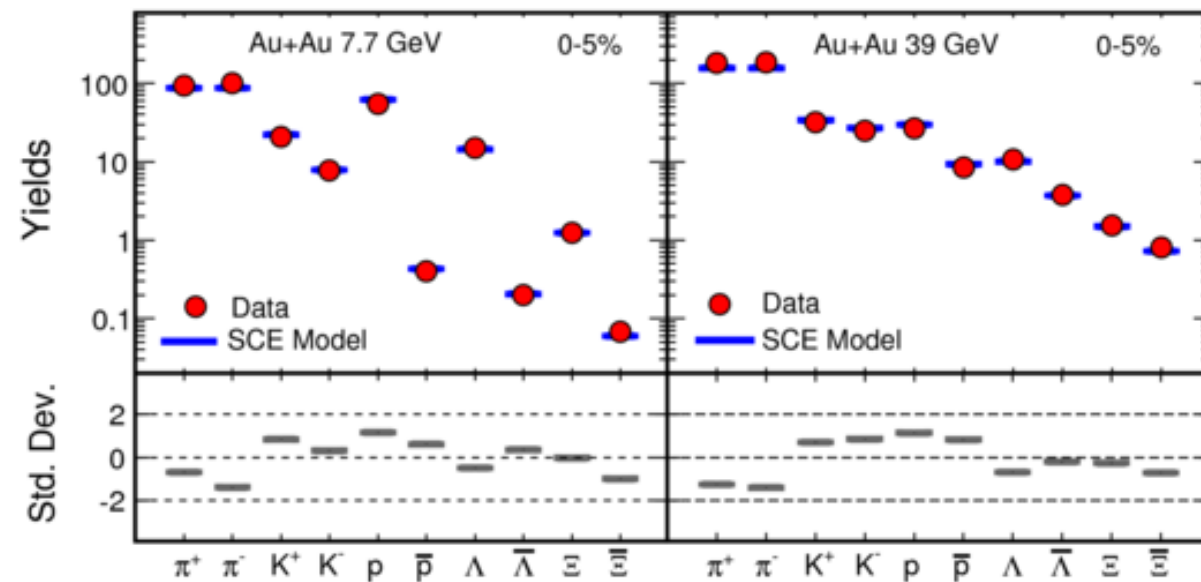
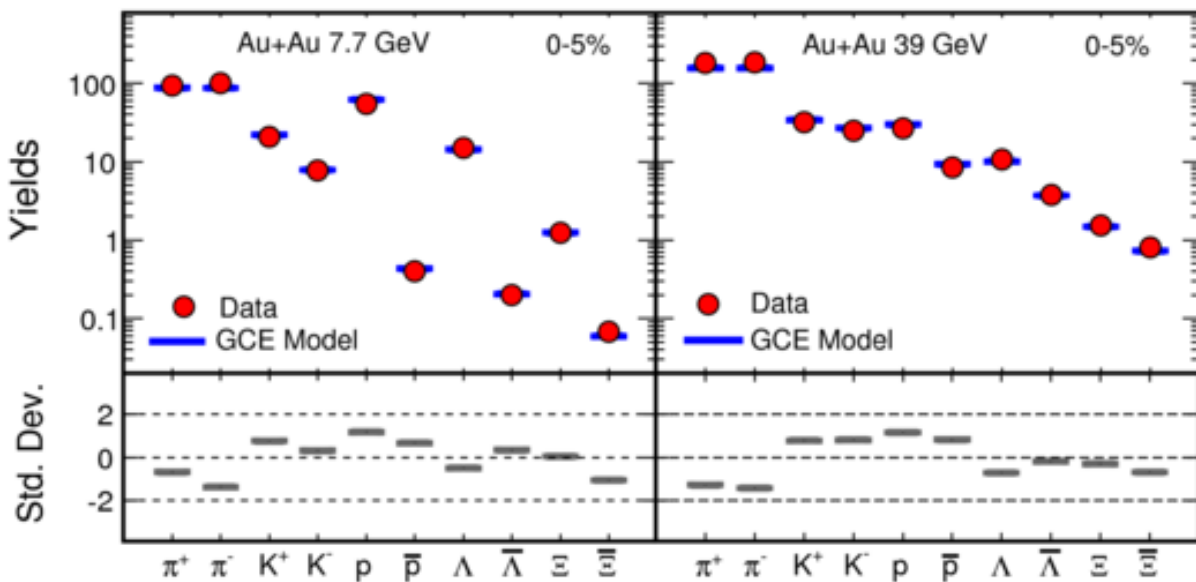
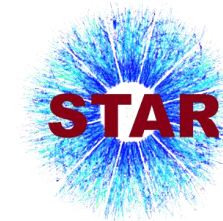
$$\frac{d^2 N}{2\pi p_T dp_T dy} \propto \left(1 + \frac{m_T - m_0}{nT}\right)^{-n}$$

Blast-wave fit

$$\frac{d^2 N}{2\pi p_T dp_T dy} \propto \int_0^R r dr m_T I_0\left(\frac{p_T \sinh \rho(r)}{T}\right) \times K_1\left(\frac{m_T \cosh \rho(r)}{T}\right)$$



# Comparison to thermal model predictions

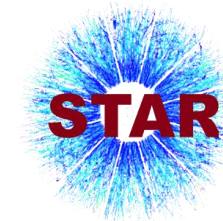


Grand Canonical Ensemble – B, Q and S are conserved on average  
 Canonical Ensemble – exact conservation of B, Q and S  
 Strangeness Canonical Ensemble – exact conservation of S

Blast-wave fits for particle spectra

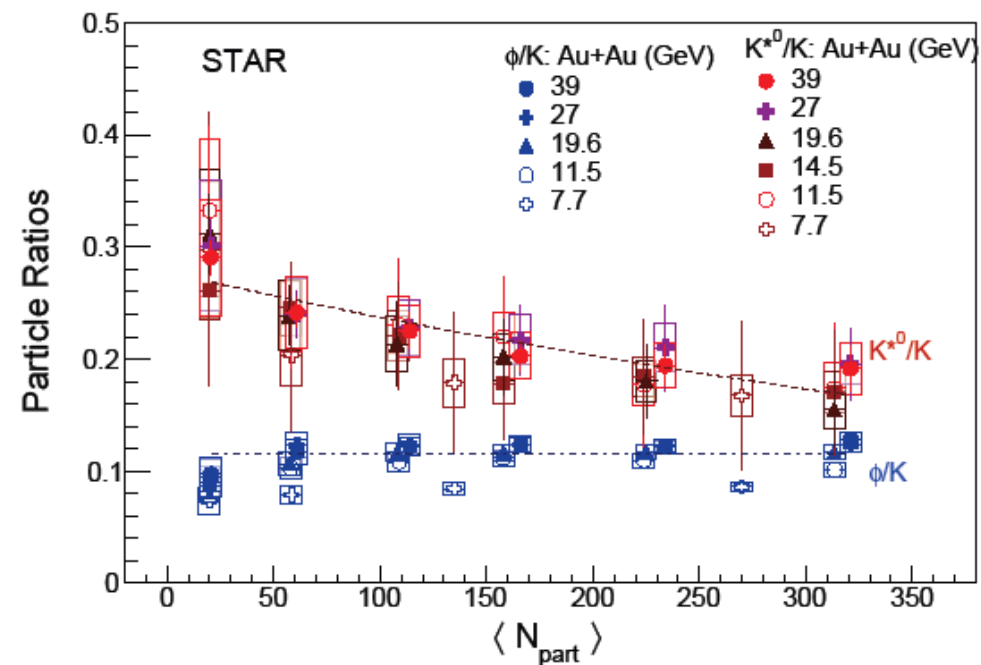
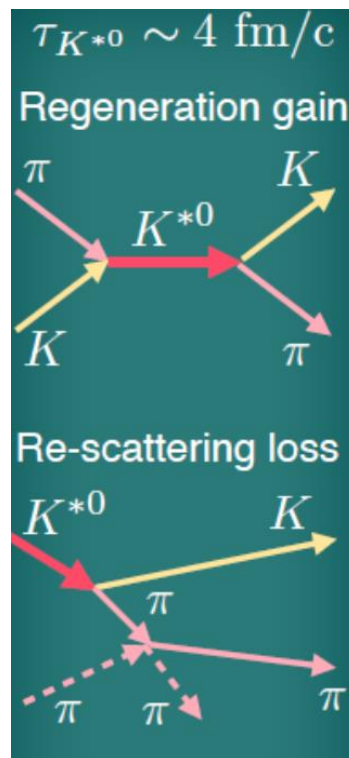
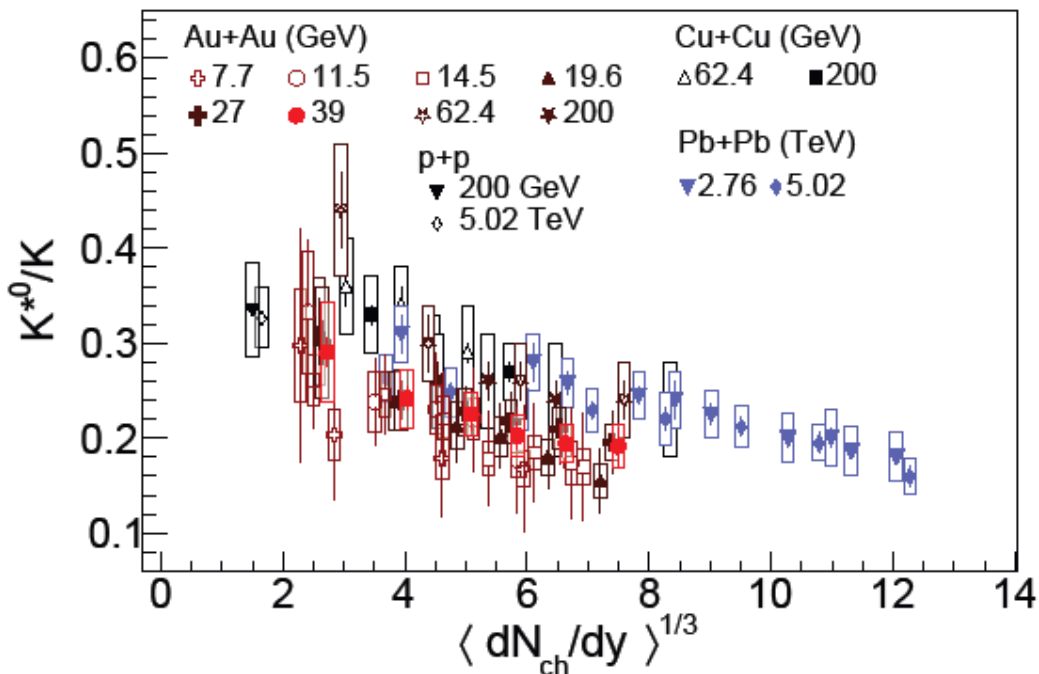
$$\frac{d^2 N}{2\pi p_T dp_T dy} \propto \int_0^R r dr m_T I_0 \left( \frac{p_T \sinh \rho(r)}{T} \right) \times K_1 \left( \frac{m_T \cosh \rho(r)}{T} \right)$$

# Hidden vs. open strangeness production

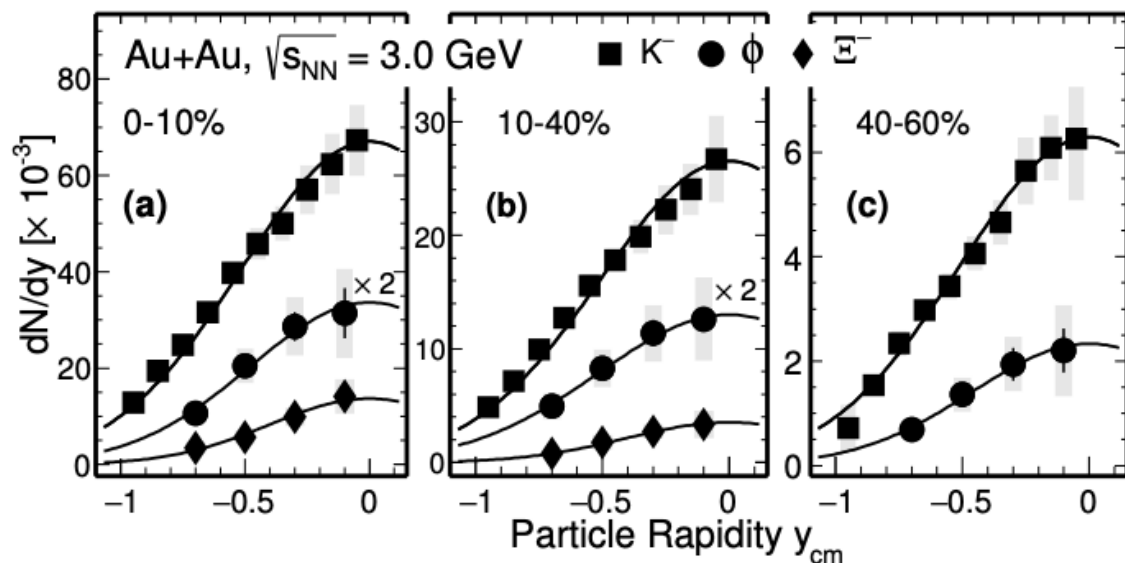
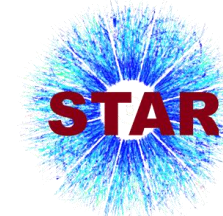


Ratio  $K^{*0}$  to  $K$  from BES data suggests re-scattering loss in medium due to shorter lifetime of  $K^{*0}$

The  $K^{*0}/K$  ratio shows a centrality dependence and follows the same trend among different collision energies. On the contrary, the  $\phi/K$  ratio is mostly independent of centrality.



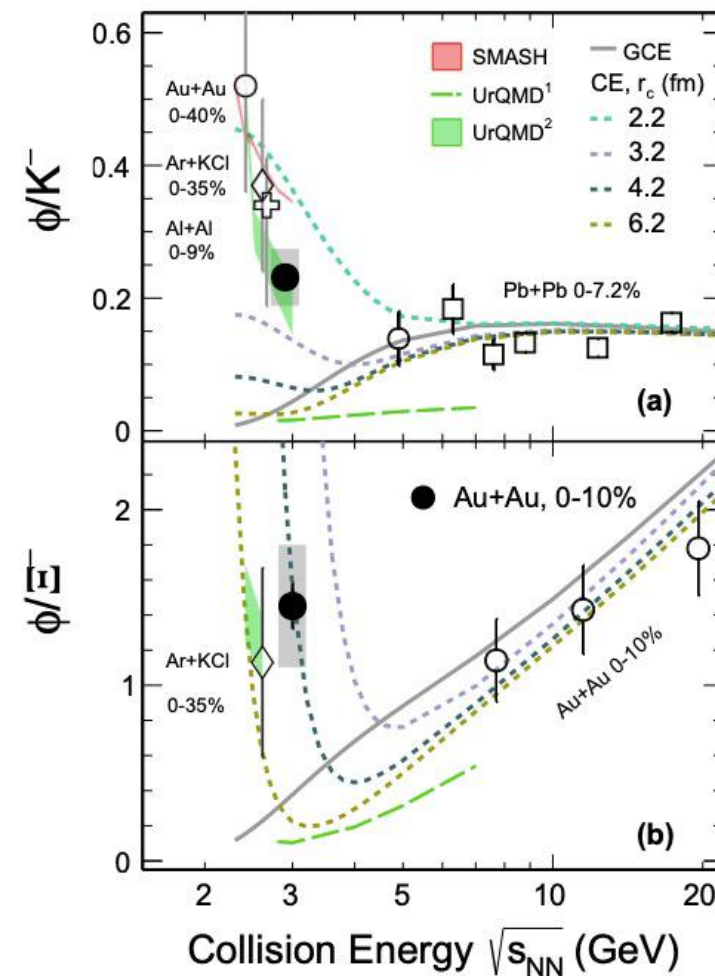
# Hidden vs. open strangeness production



The thermal model with grand canonical ensemble (GCE) under-predicts the ratios

The canonical ensemble (CE) calculations reproduce the ratios with a correlation length of 3-4 fm

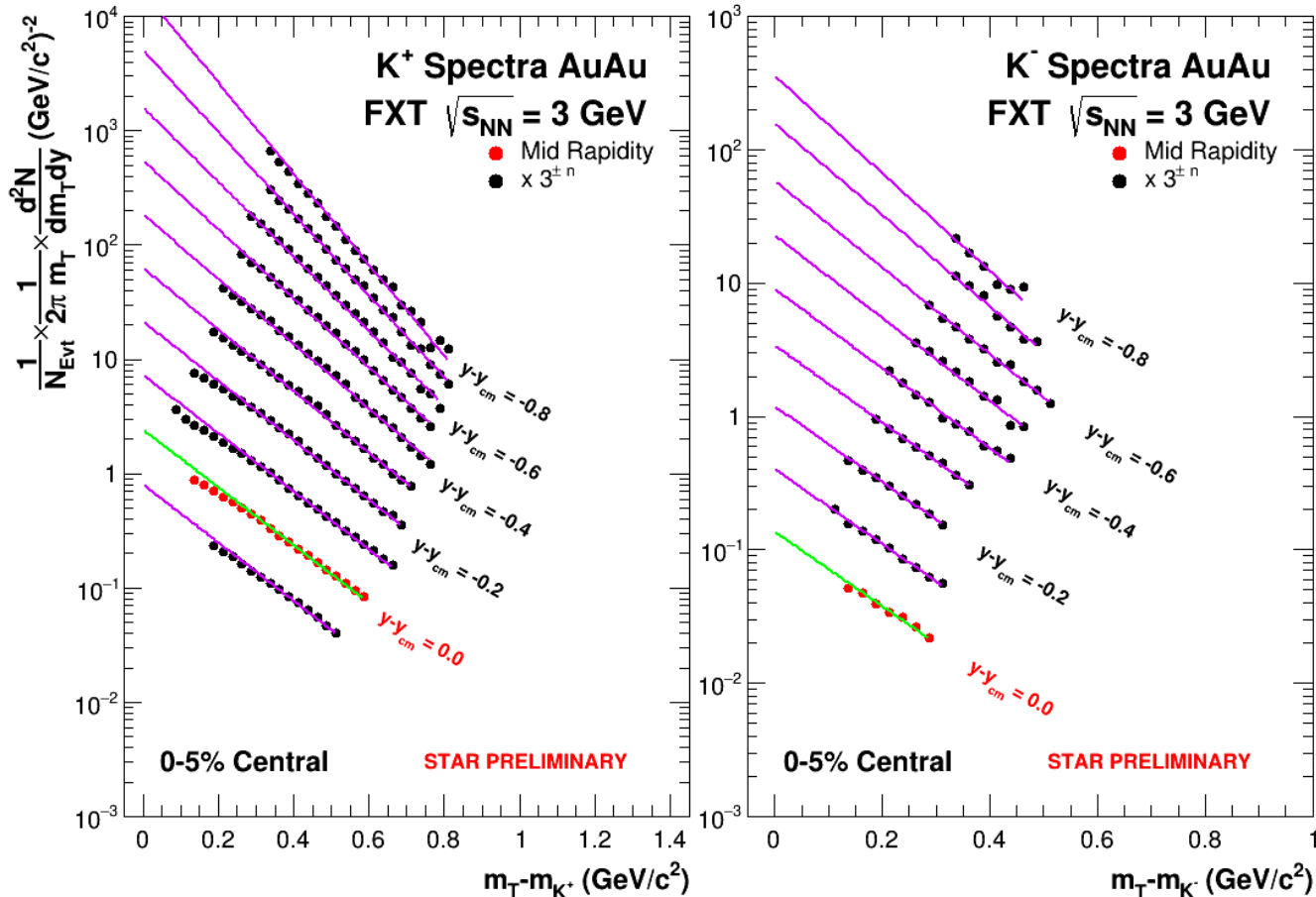
These observations imply that strange particles are produced in a system of high baryon density causing the small correlation length



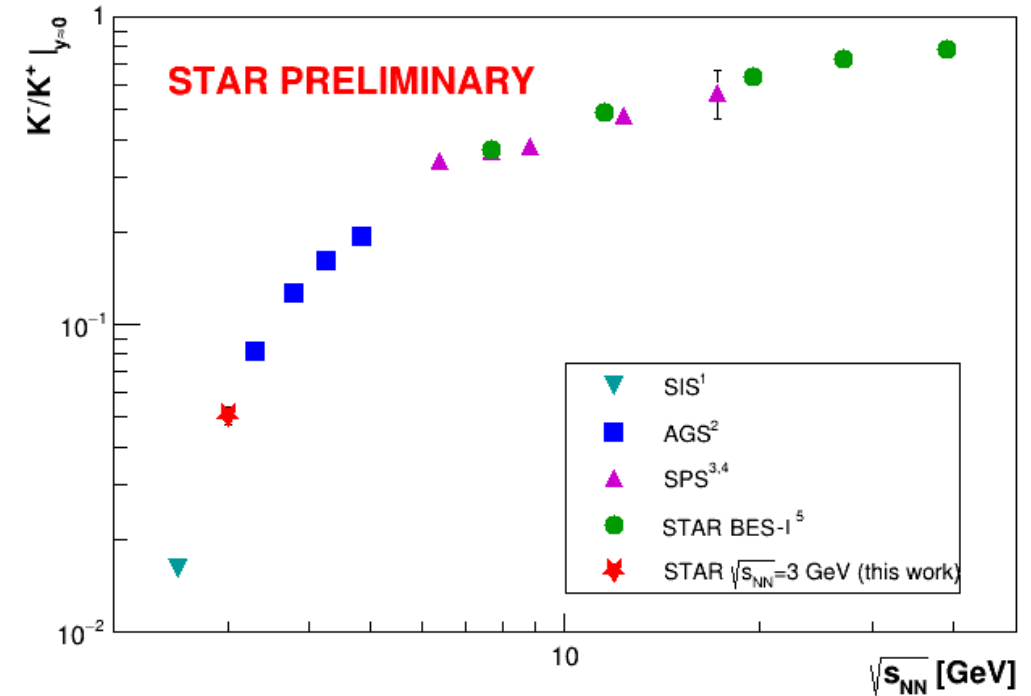
# Charged kaon production at 3 GeV



Kaon spectra near midrapidity described well with  $m_T$  exponential function since Bose-Einstein enhancement and radial flow effects mostly cancel

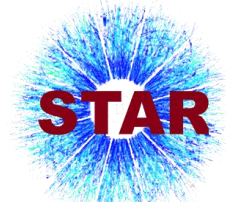


K<sup>-</sup>/K<sup>+</sup> ratio at midrapidity is affected by baryon stopping

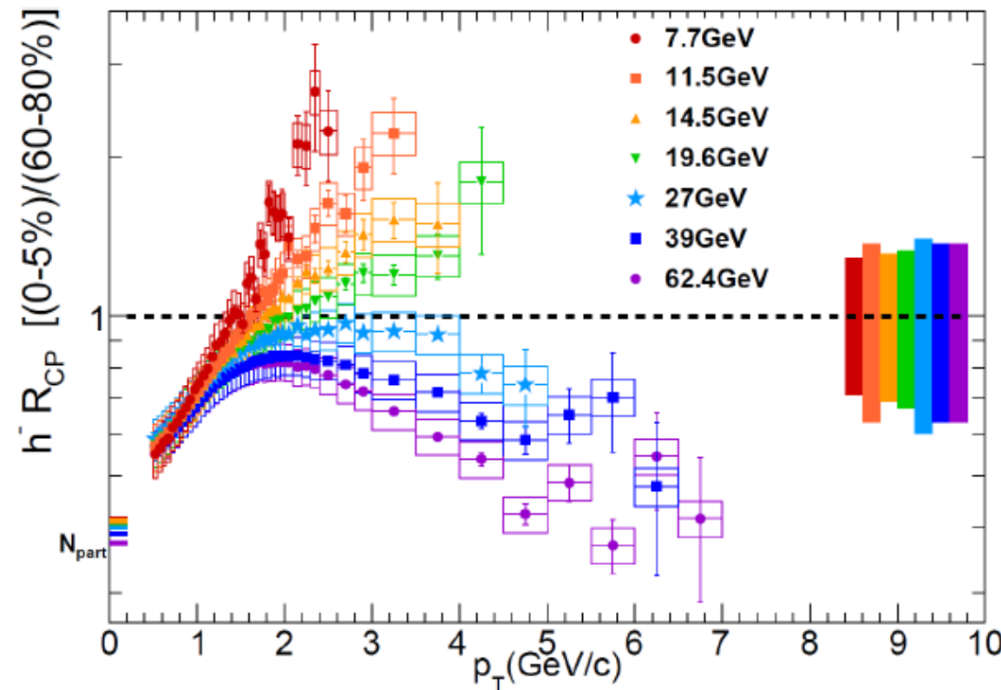


- 1 A. Forster et al. (KaoS Collaboration), J. Phys. G **28**, 2011 (2002)
- 2 L. Ahle et al. (E866 and E917 Collaborations), Phys. Lett. B **490**, 53 (2000)
- 3 C. Alt et al. (NA49 Collaboration), Phys. Rev. C **77**, 024903 (2008)
- 4 S. Afanasiev et al. (NA49 Collaboration), Phys. Rev. C **66**, 054902 (2002)
- 5 L. Adamczyk et al. (STAR Collaboration), Phys. Rev. C **96**, 044904 (2017)

# Nuclear modification in the medium

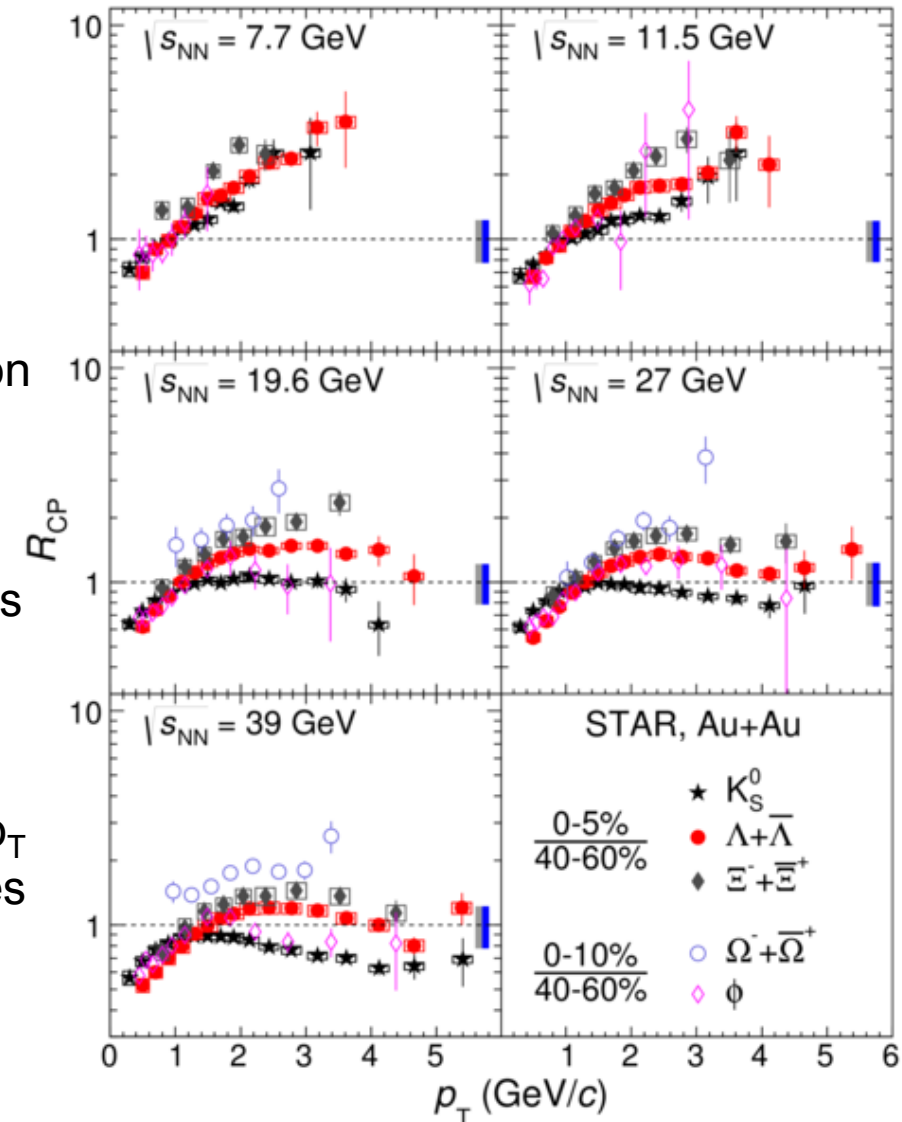


$$R_{cp} = \frac{d^2 N dp_t d\eta / \langle N_{coll} \rangle (central)}{d^2 N dp_t d\eta / \langle N_{coll} \rangle (peripheral)}$$

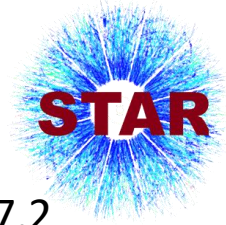


$R_{cp}$  has two regimes in the behavior depending on the collision energy:  
 decrease of particle production with high  $p_T$  in central collisions at high energies  
 smooth growth of particle production in central collisions at low collision energies.

High statistics of BES-II will allow to measure  $R_{cp}$  in high  $p_T$  region at low collision energies

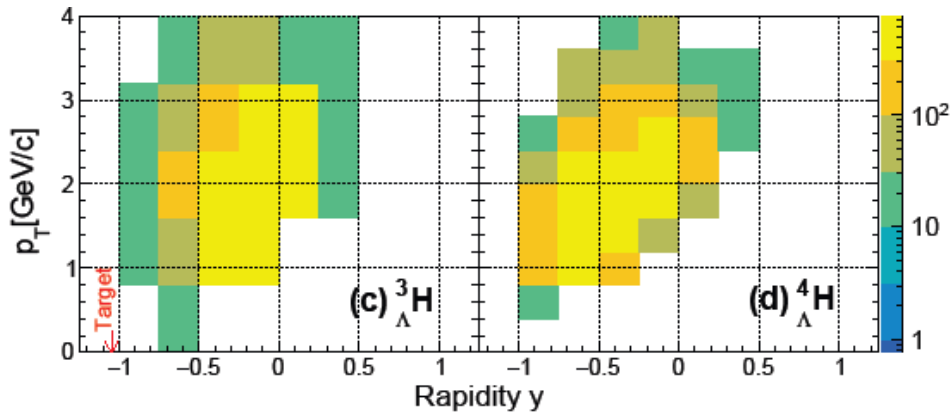
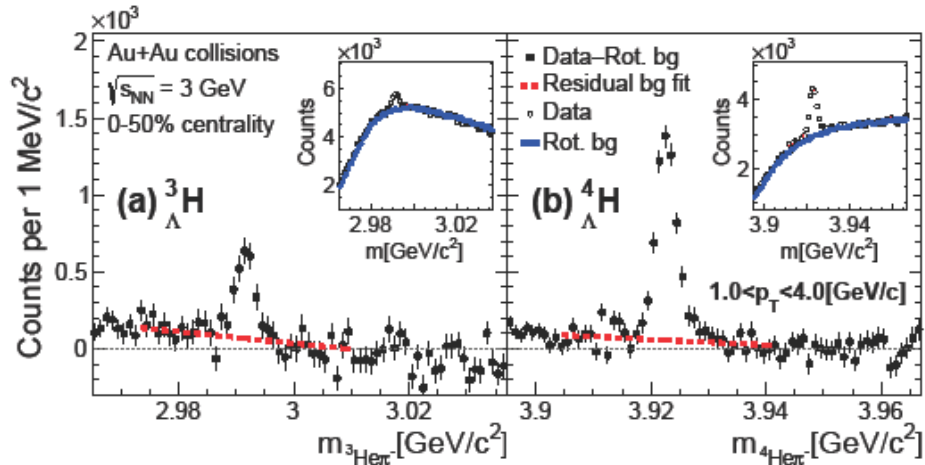


# Hypernuclei production



300M Au+Au data without iTPC and eTOF

Candidate reconstruction via invariant mass in two body decay

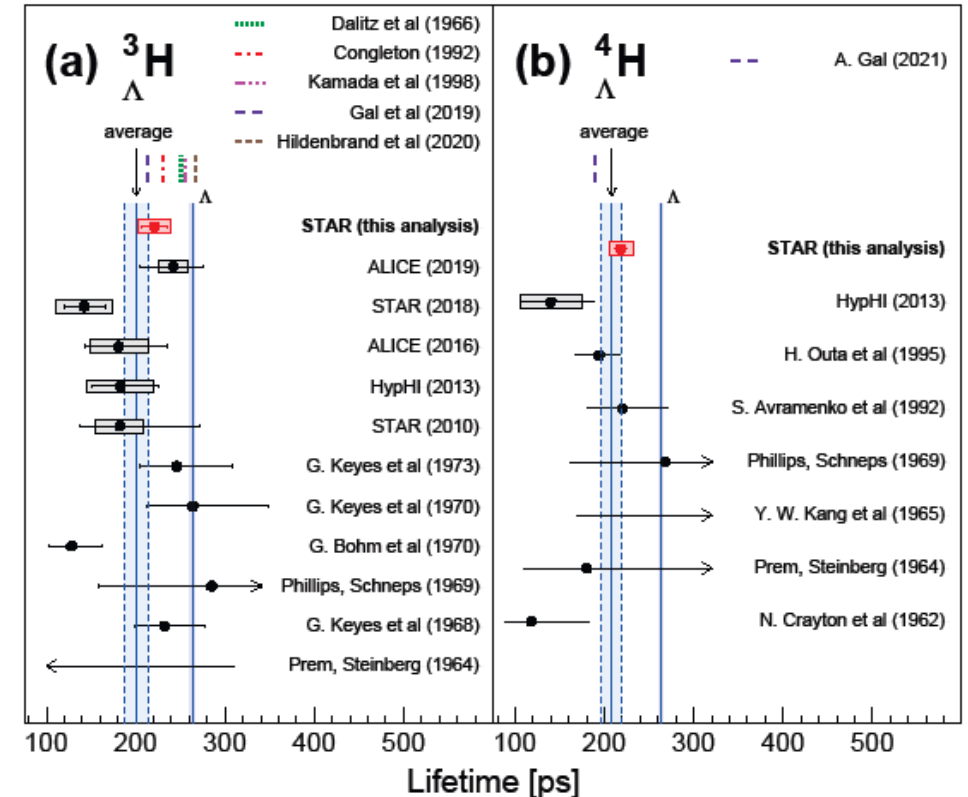
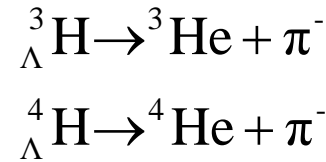


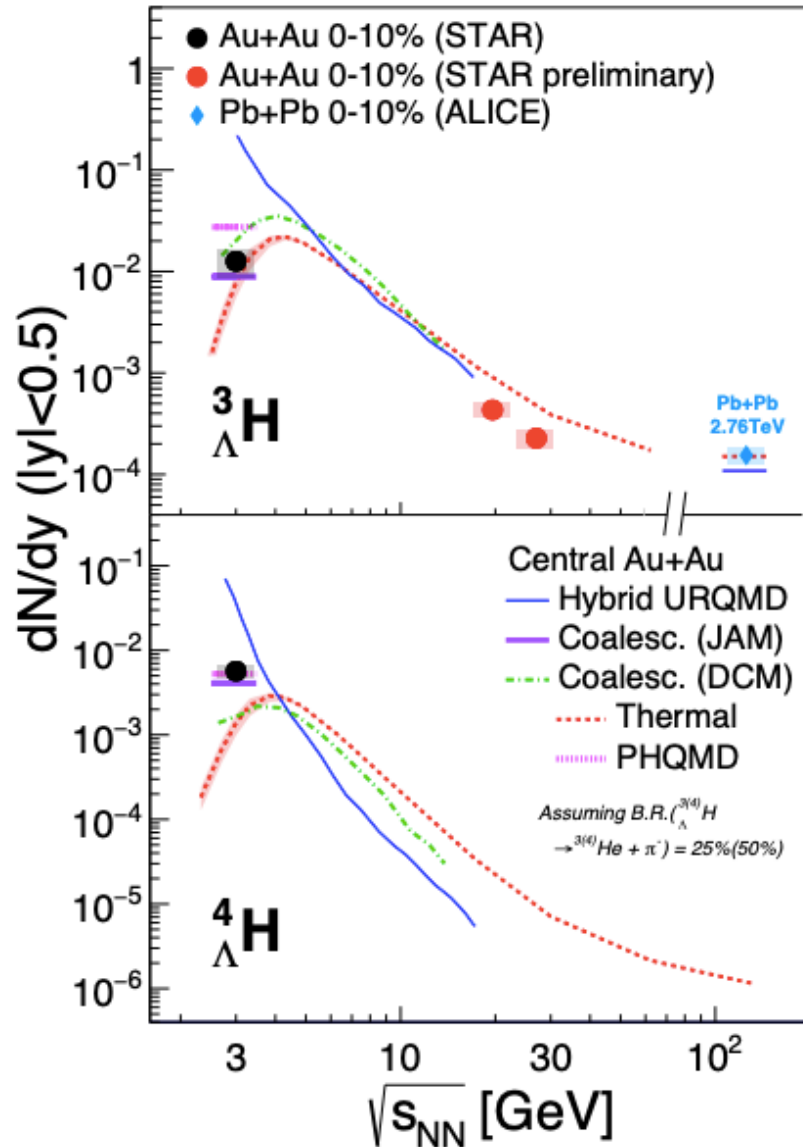
Lifetime measurements are consistent with previous measurements and have higher precision

Measured lifetime results at  $\sqrt{s_{NN}} = 3.0$  and  $7.2$  GeV are in a good agreement with each other  
The combined results are

$$\tau({}^3_{\Lambda}\text{H}) = 221 \pm 15(\text{stat.}) \pm 19(\text{syst.}) \text{ ps.}$$

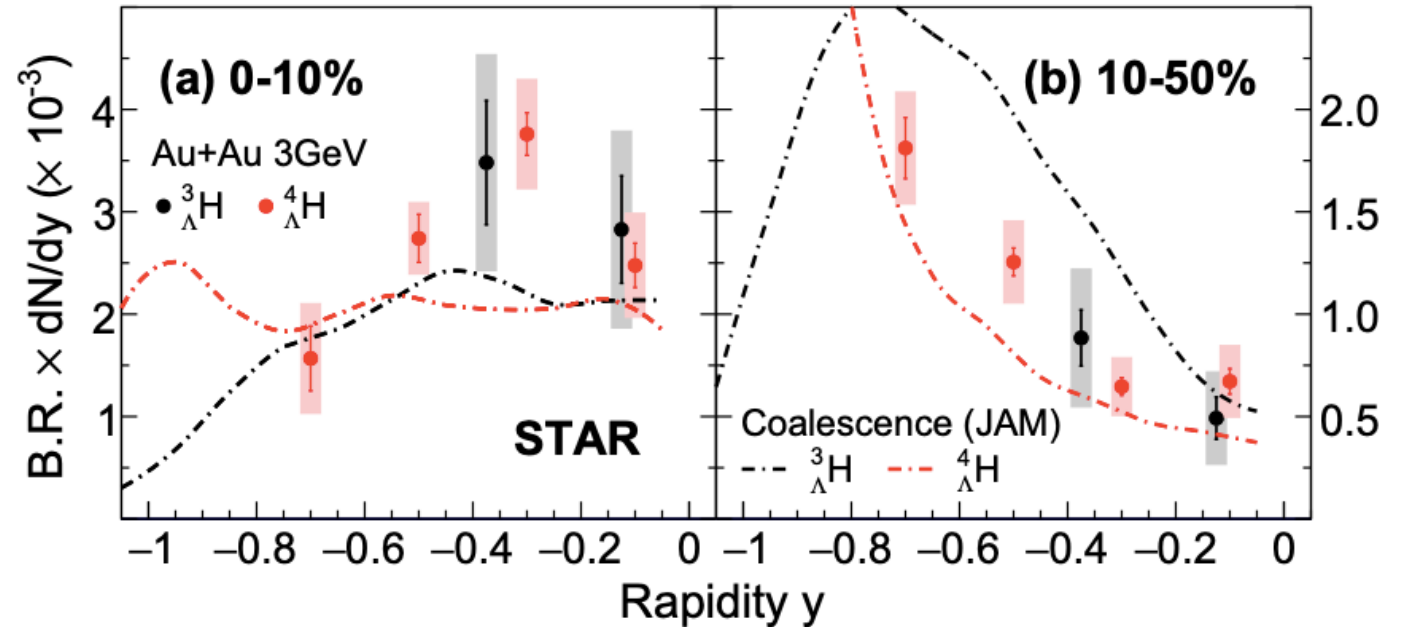
$$\tau({}^4_{\Lambda}\text{H}) = 218 \pm 6(\text{stat.}) \pm 13(\text{syst.}) \text{ ps.}$$



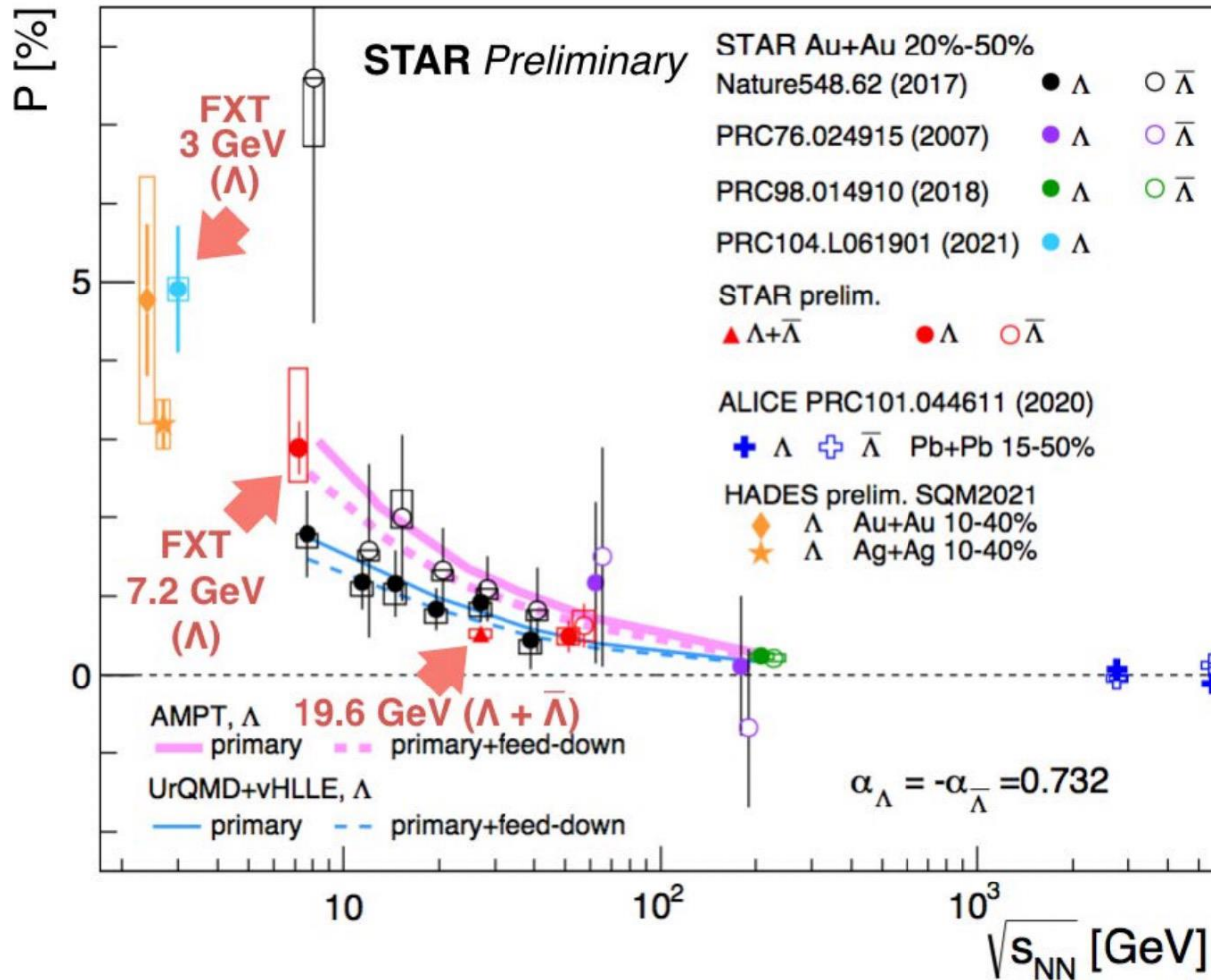


Hypertriton yields follow the thermal model prediction

Hyper-H4 yields are under predicted by the thermal model



# Global hyperon polarization measurements



Global hyperon polarization over a large range of collision energy is measured and can be described by hydrodynamic and transport models with intense fluid vorticity of the QGP

The observation of substantial polarization in these collisions may require a reexamination of the viscosity of any fluid created in the collision, of the thermalization timescale of rotational modes, and of hadronic mechanisms to produce global polarization.

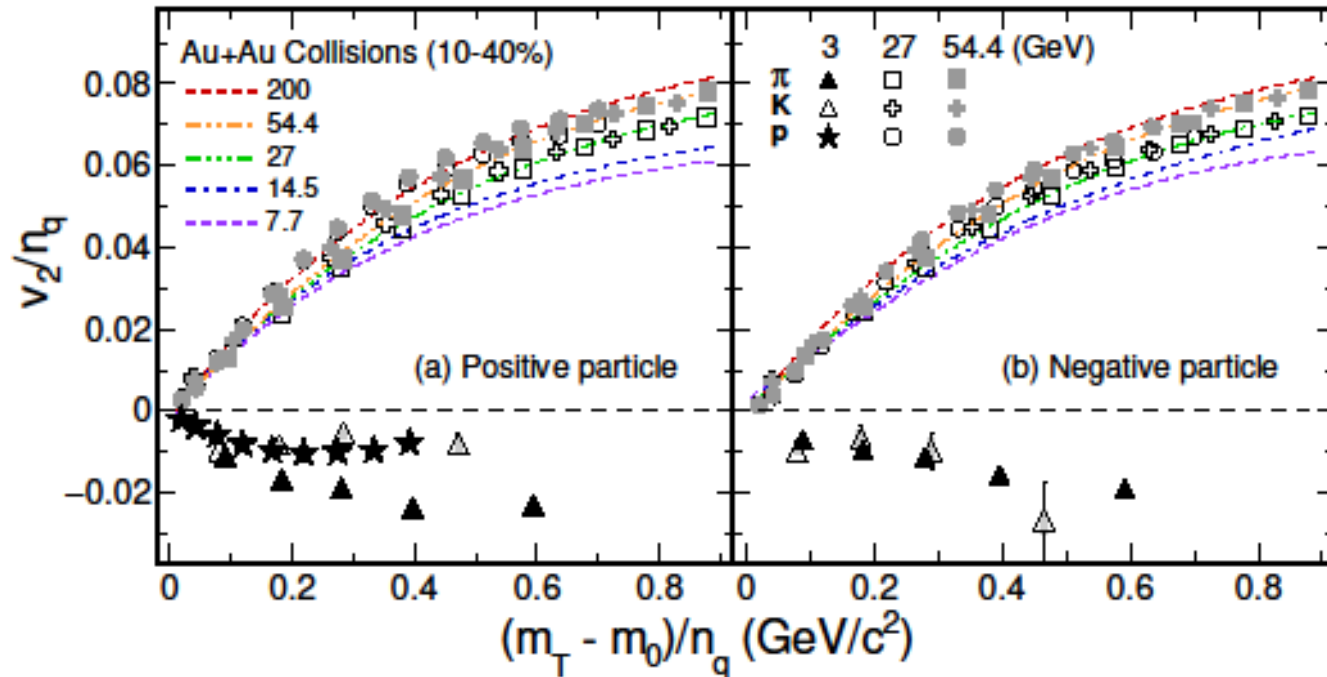
$$\frac{dN}{d \cos \theta^*} = \frac{1}{2} \left( 1 + \alpha_H |\vec{\mathcal{P}}_H| \cos \theta^* \right)$$



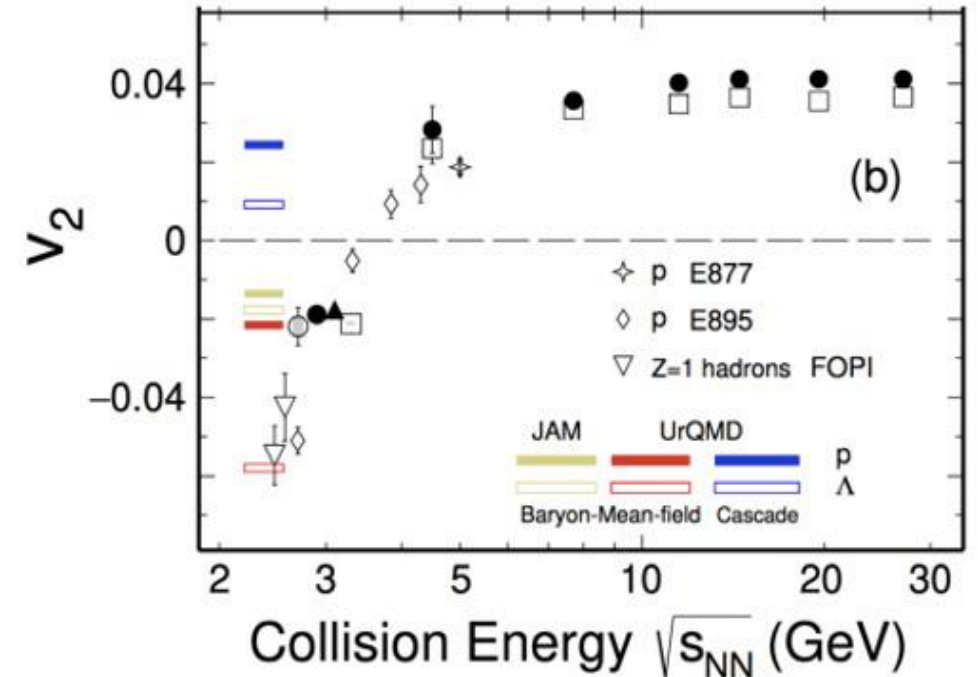
# Elliptic flow at 3 GeV



Elliptic flow is negative (squeeze-out) at 3 GeV, as expected from the previous AGS data



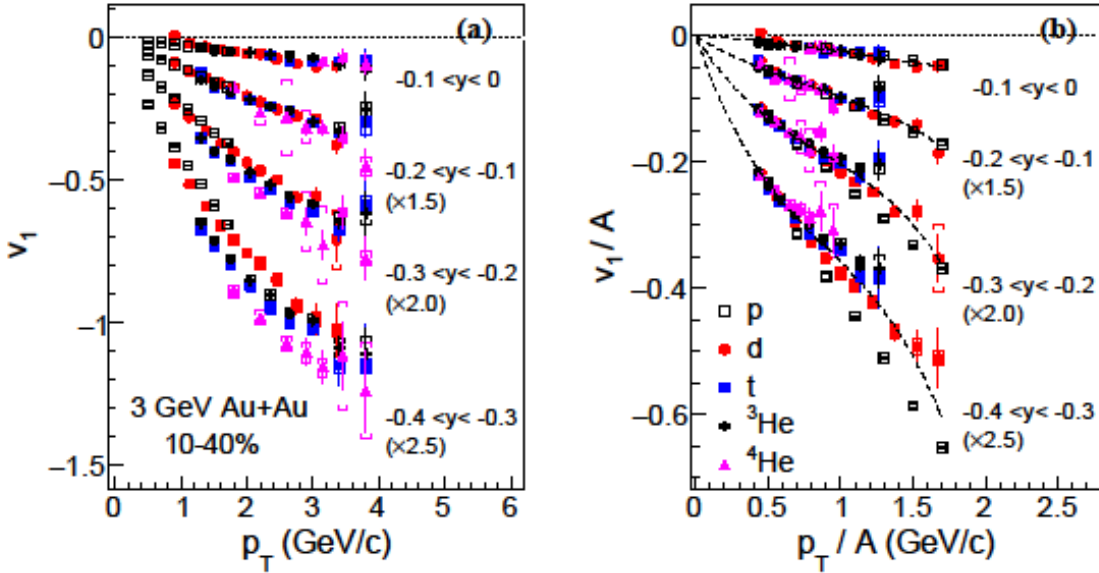
The quark number scaling has been used at higher energies as a signature of the QGP. At 3 GeV, the scaling is broken down e.g. hadronic gas (not QGP).



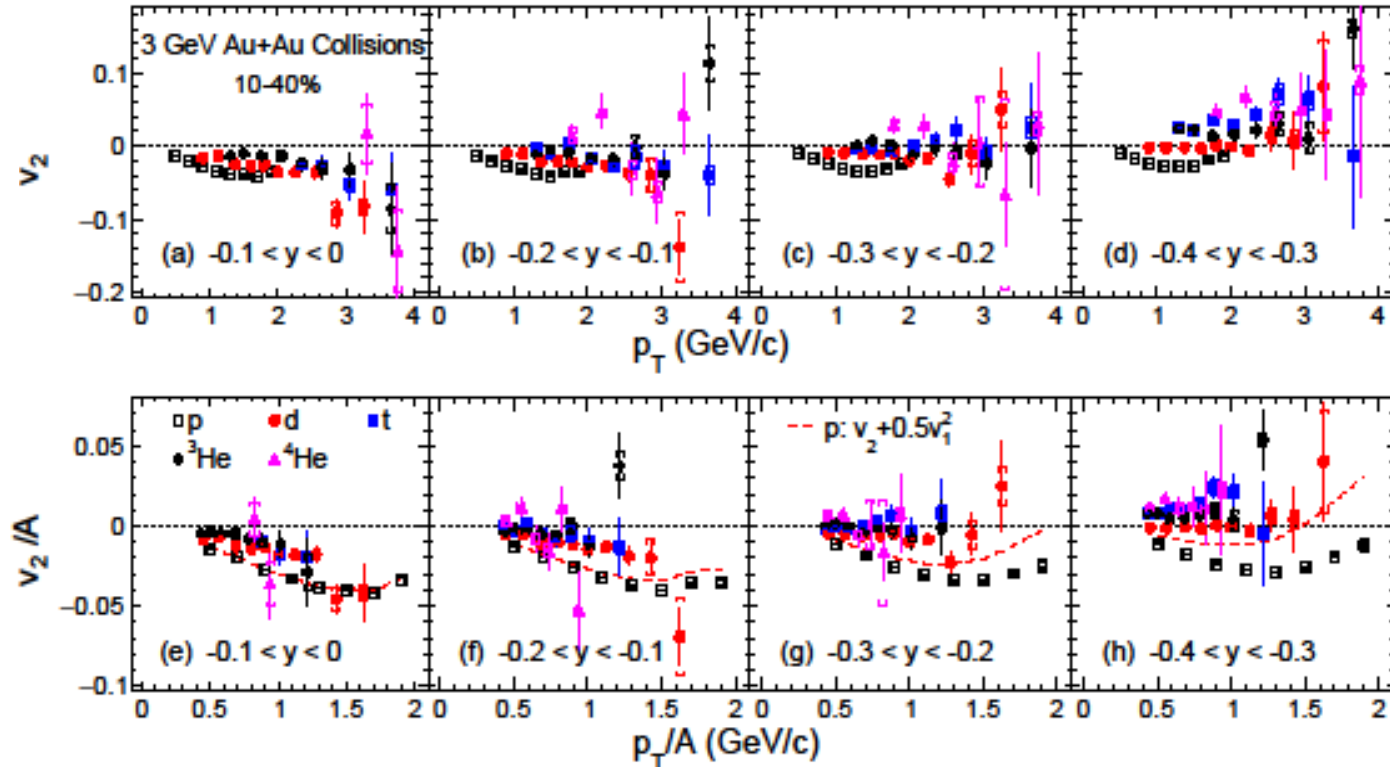
# Collective flow of light nuclei



$v_1$  and  $v_2$  values are negative for all measured light nucleus species except for  $v_2$  within  $-0.4 < y < -0.3$



This indicates that no A scaling is observed in these data for light nucleus  $v_2$  at 3 GeV. The A scaling has been observed for  $p_T/A < 1.5$  GeV/c in higher energy Au+Au collisions at  $\sqrt{s_{NN}} = 7.7 - 200$  GeV



The  $v_1$  scaling behavior suggests the light nuclei are formed via nucleon coalescence

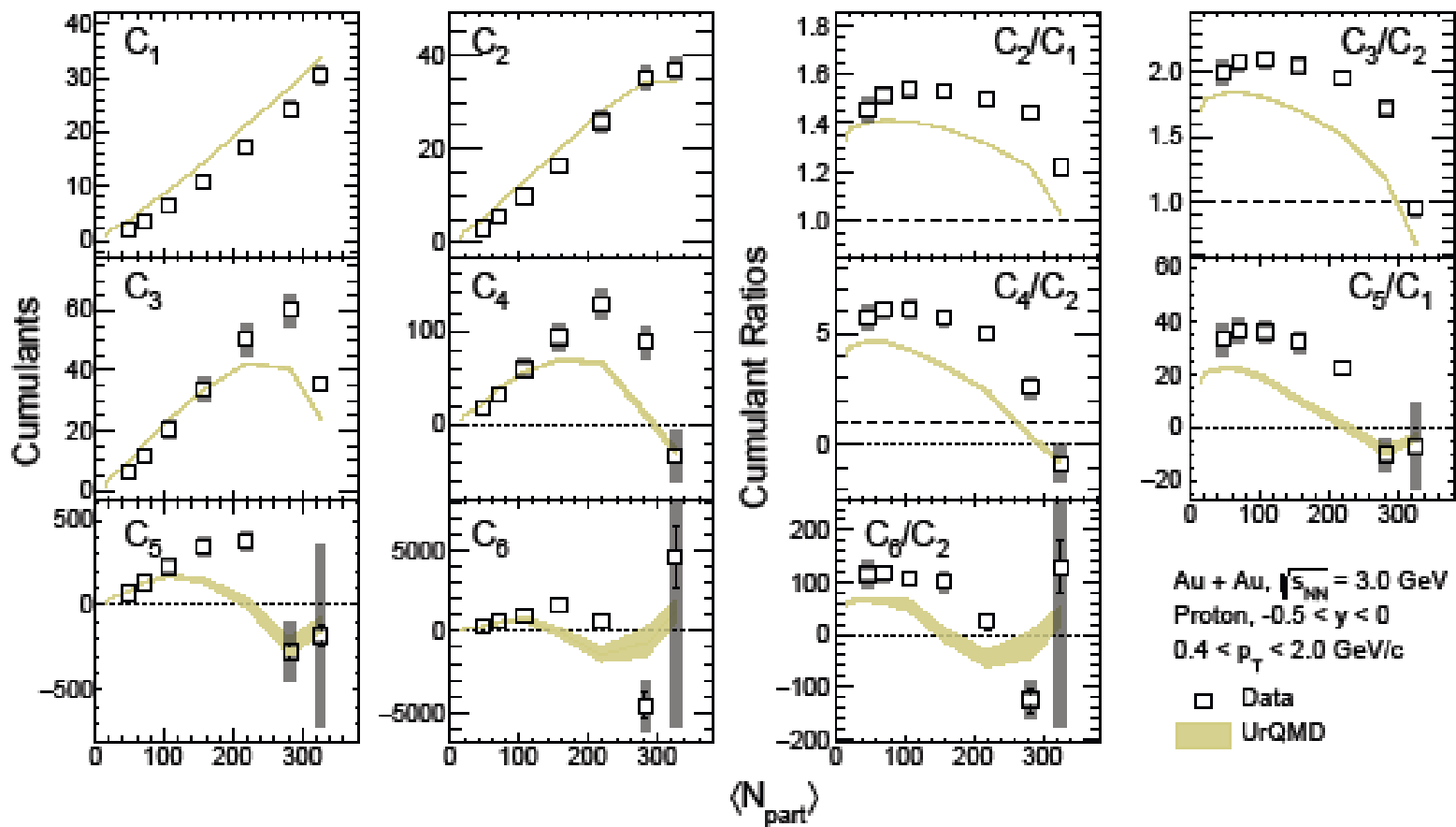
The scaling worsens for  $p_T/A > 1$  GeV/c in the range  $-0.4 < y < -0.3$ , where simple coalescence may not apply

Increasing contamination of target-rapidity ( $y = -1.045$ ) fragments may also play a role

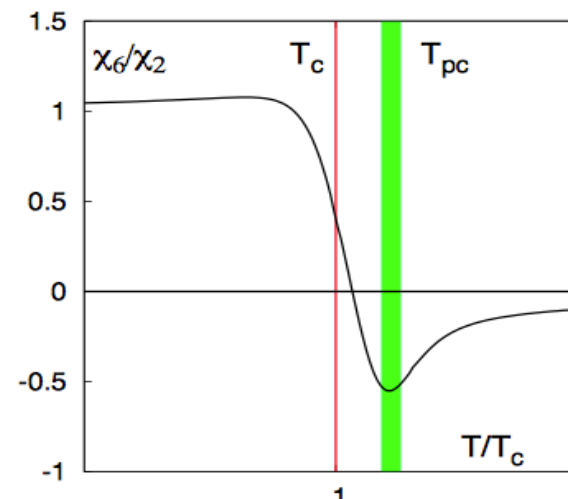
# Higher-order cumulants at 3 GeV



## Cumulants of proton and its ratios at 3 GeV



Higher-order cumulant ratios  $C_4/C_2$ ,  $C_5/C_1$ , and  $C_6/C_2$  in most central events appear least affected by volume fluctuations in the 3 GeV Au+Au collisions



Susceptibility ratios fluctuate near the CP. It can be measured via cumulants of net-protons

$$C_1 = \langle N \rangle$$

$$C_2 = \langle (\delta N)^2 \rangle$$

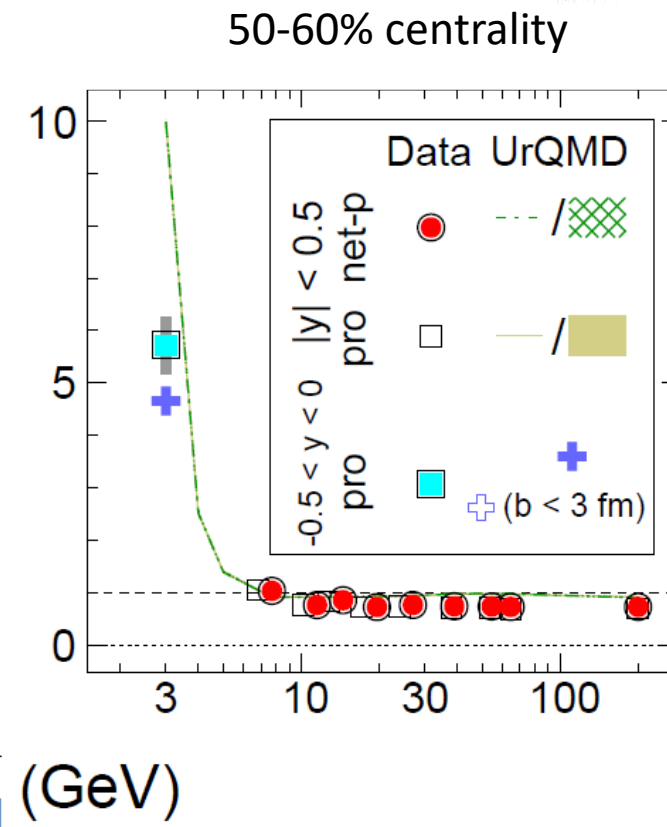
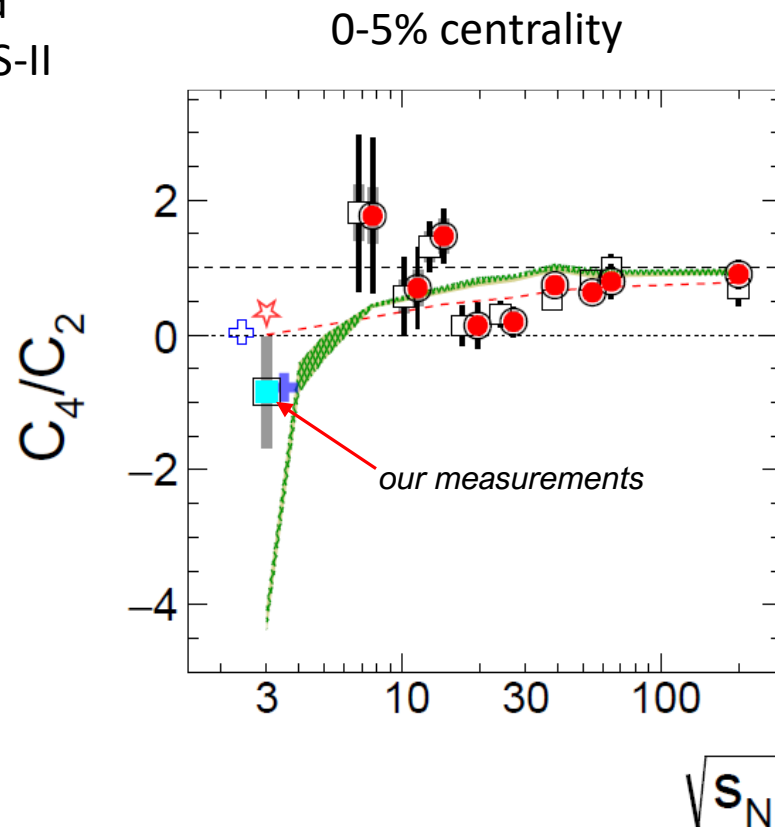
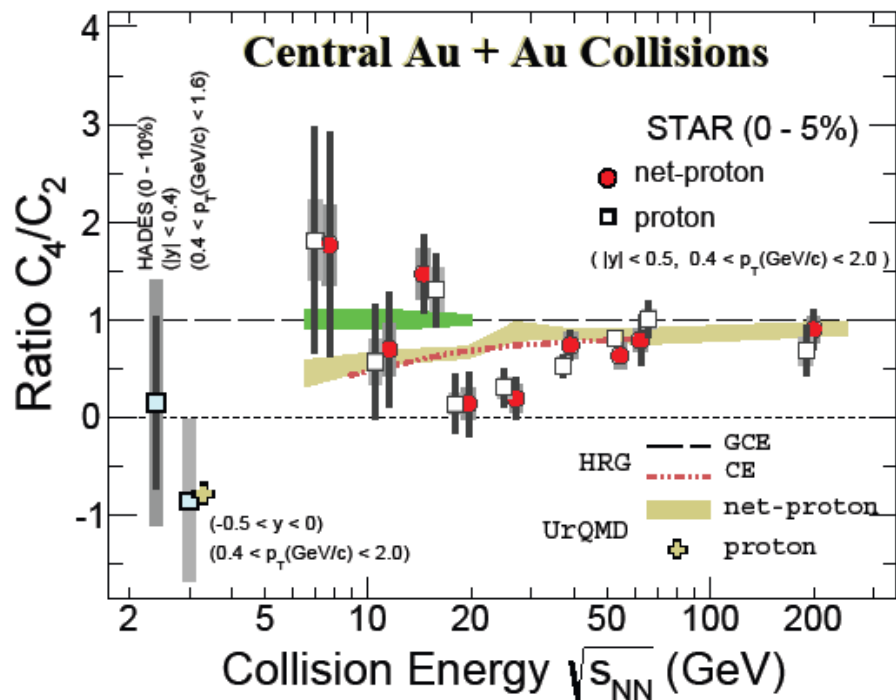
$$C_3 = \langle (\delta N)^3 \rangle$$

$$C_4 = \langle (\delta N)^4 \rangle - 3 \langle (\delta N)^2 \rangle^2$$

# Energy dependence of net-proton cumulant ratio

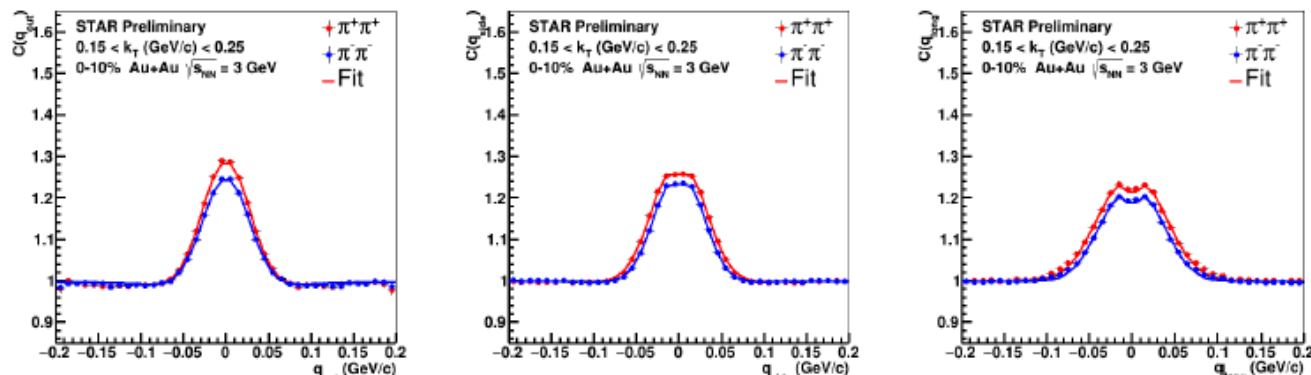
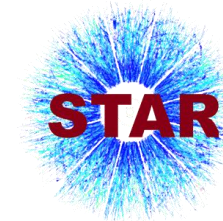


Previous measurements of net-protons by STAR and HADES suggested the sign change at energies of BES-II

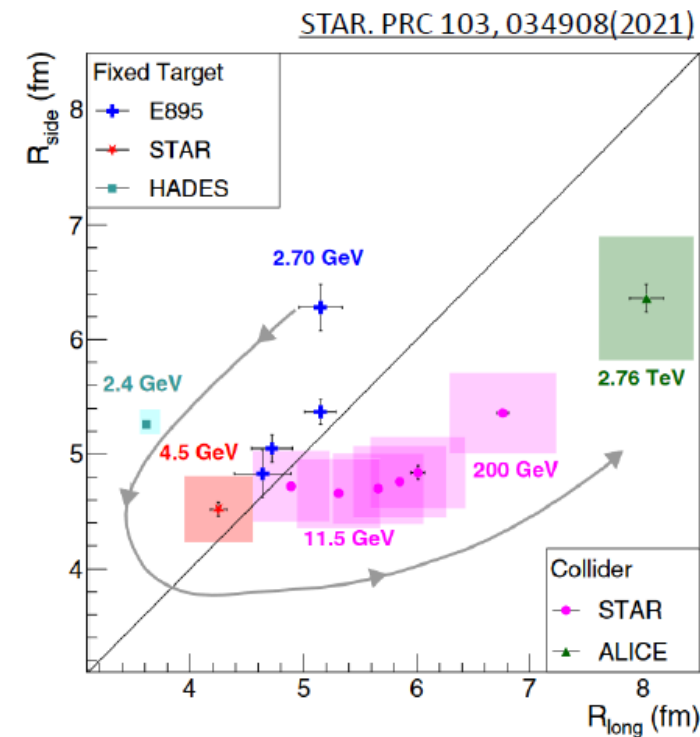
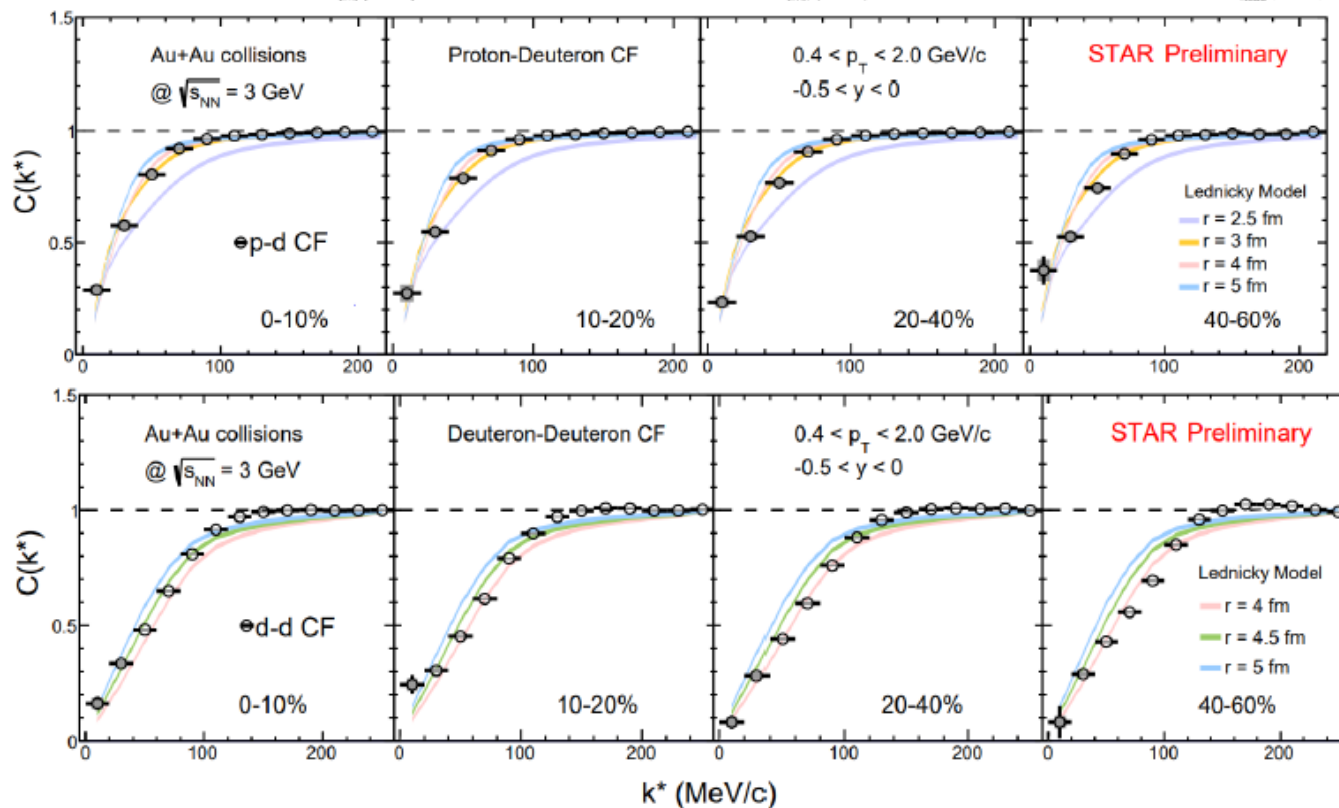


The data and results of both UrQMD and hydrodynamic models of  $C_4/C_2$  in the most central collisions at 3 GeV are consistent, which signals the effects of baryon number conservation and an energy regime dominated by hadronic interactions

# Femtoscscopy results from FXT program

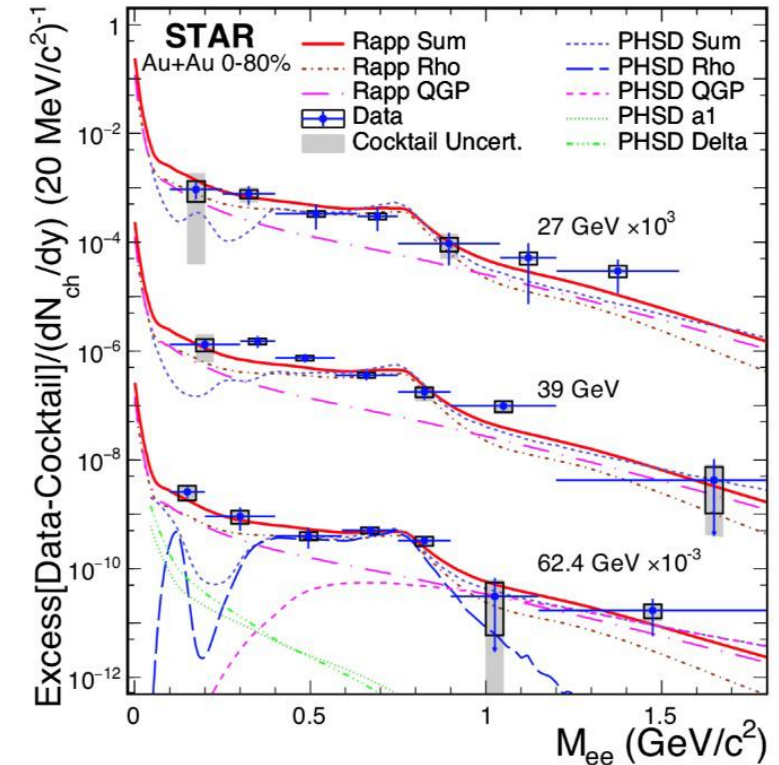
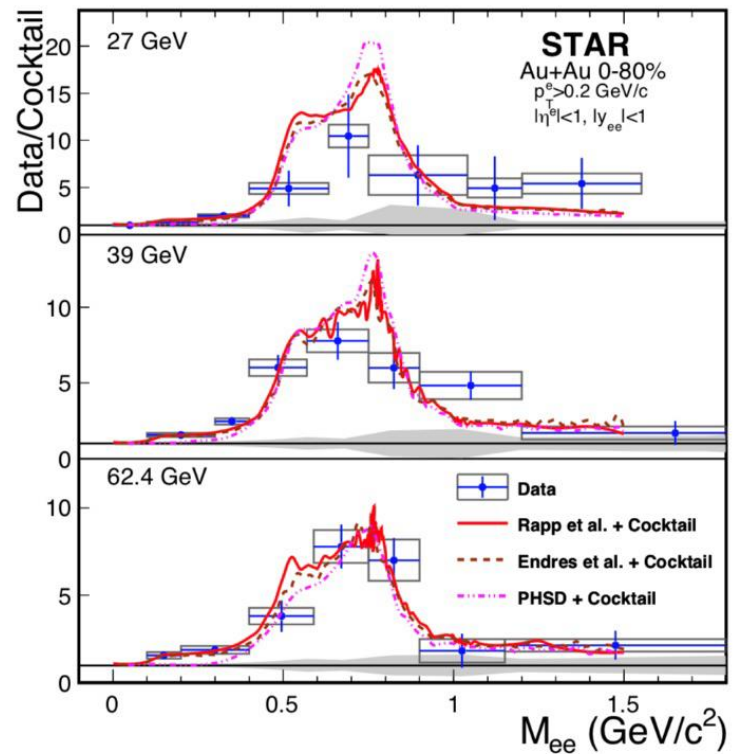
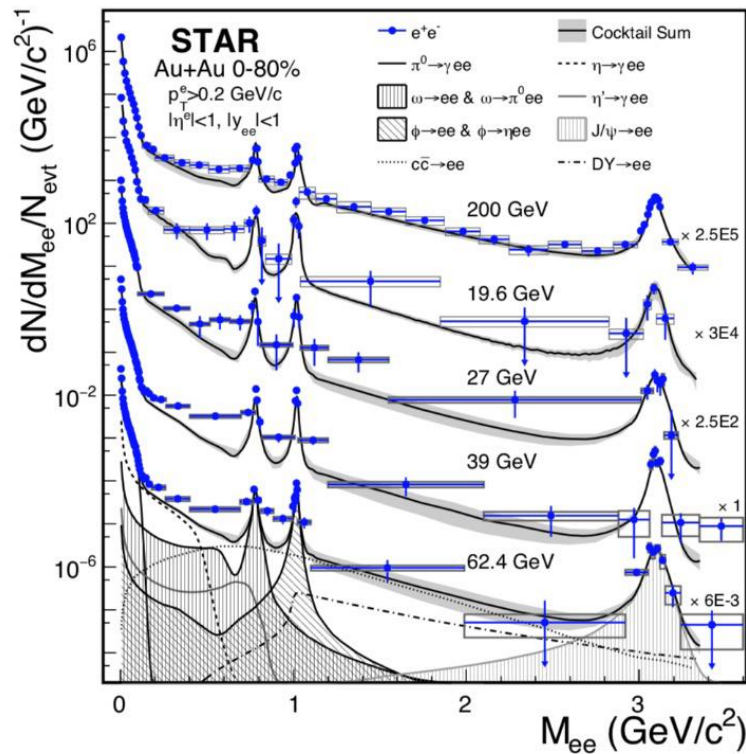


Many interesting results from low energy nuclear collisions:  $\pi\pi$ ,  $pp$ ,  $pd$ ,  $dd$ , and others provide information about particle interactions



The source shape evolves from oblate to prolate, as energy increases

# Dielectron production in BES-I



200 GeV: high yield of heavy flavor quark semi-leptonic decay  
 19.6–62.4 GeV: lack of statistics

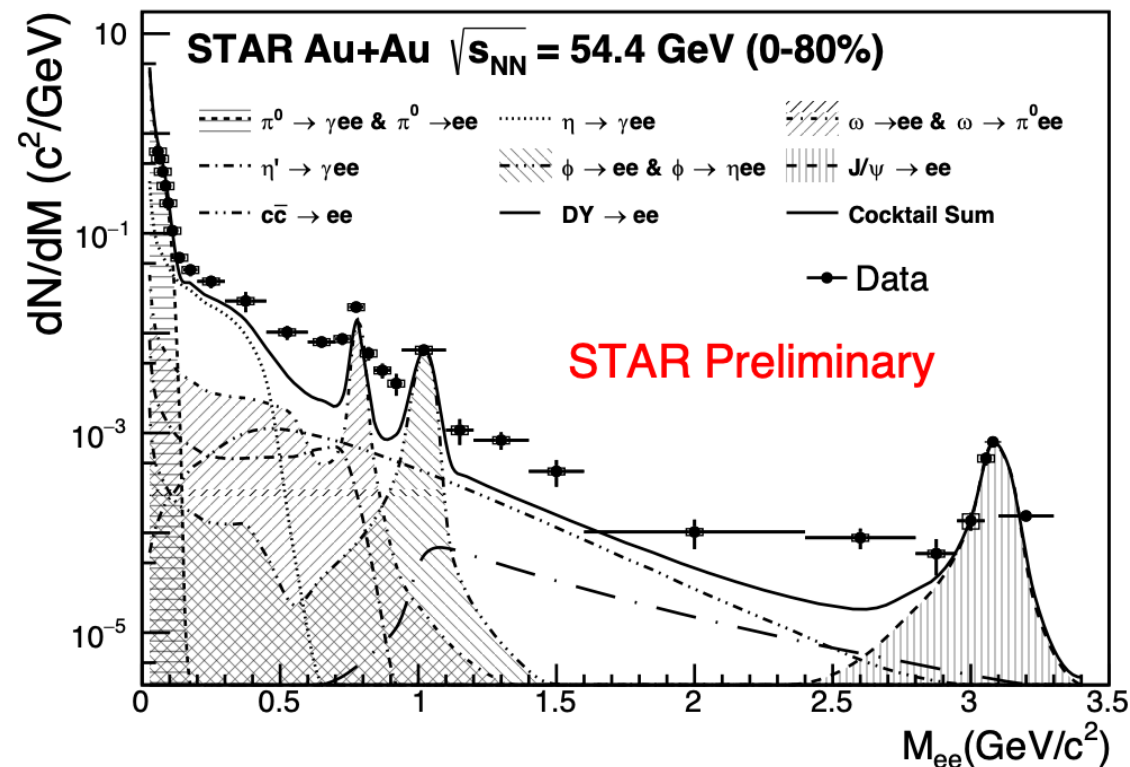
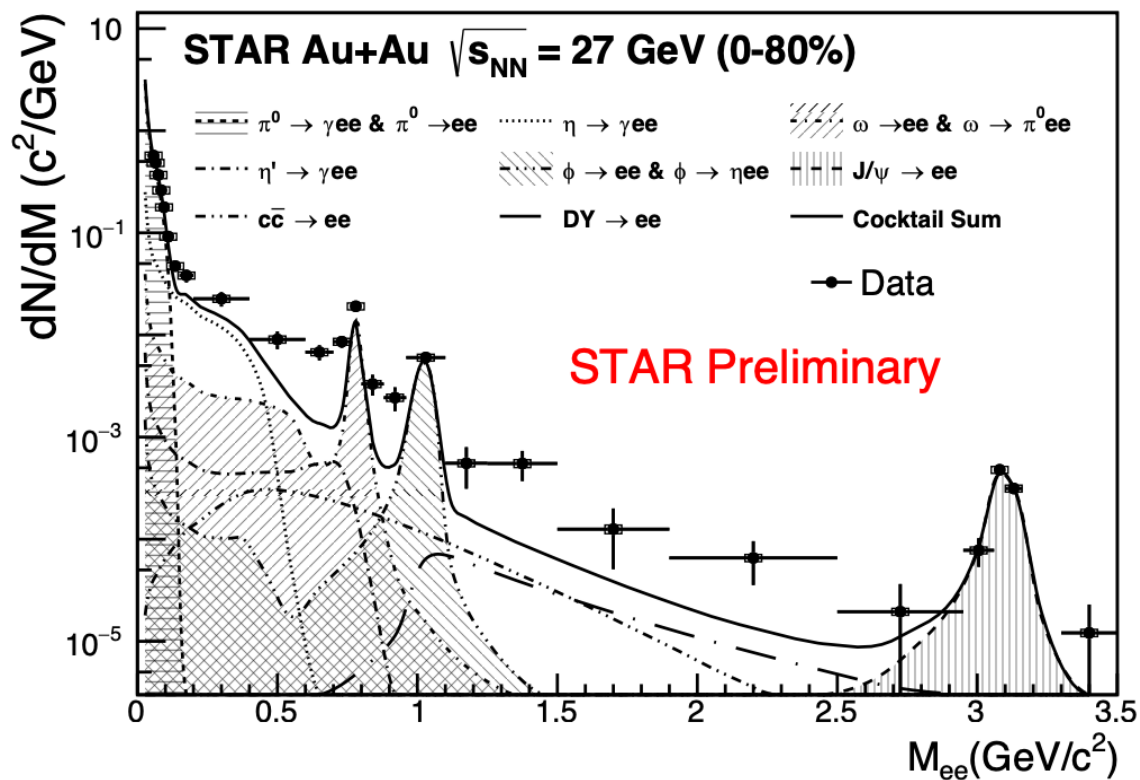
arXiv:1810.10159

Phys. Lett. B 750,64-71(2015)

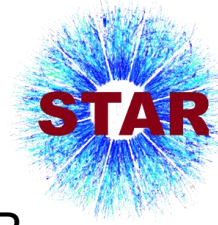
Phys. Rev. Lett. 113,022301 (2014)

Alexey Aparin, ICPPA-2022, Moscow NRNU MEPhI, 29.11–02.12.2022

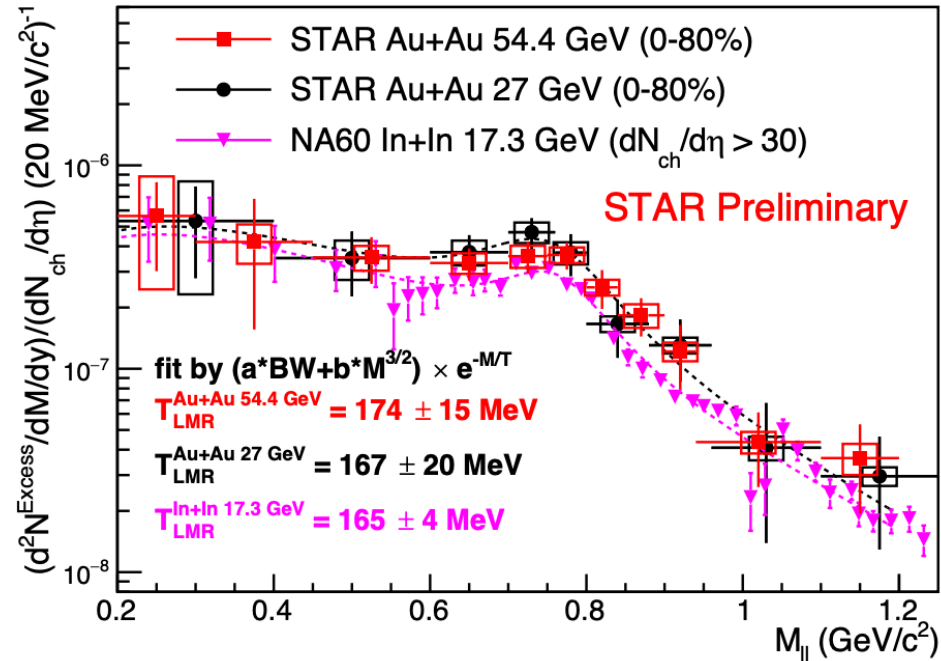
# Dielectron production at 27 and 54.4 GeV Au+Au collisions



Clear enhancement compared to  $\rho$  excluded cocktail simulation in LMR and IMR

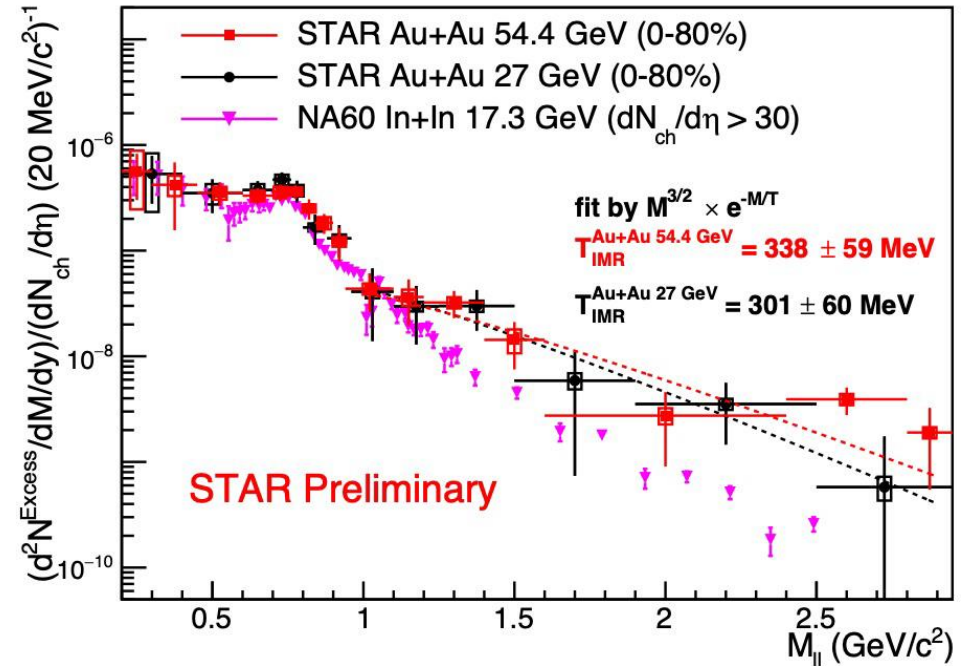


Excess dielectron spectra in 27 and 54.4 GeV Au+Au collisions and NA60 In+In collisions are similar



T extracted from low mass region around the pseudo critical temperature  $T_{pc}$  (156 MeV)

Thermal dielectrons is the major source in IMR

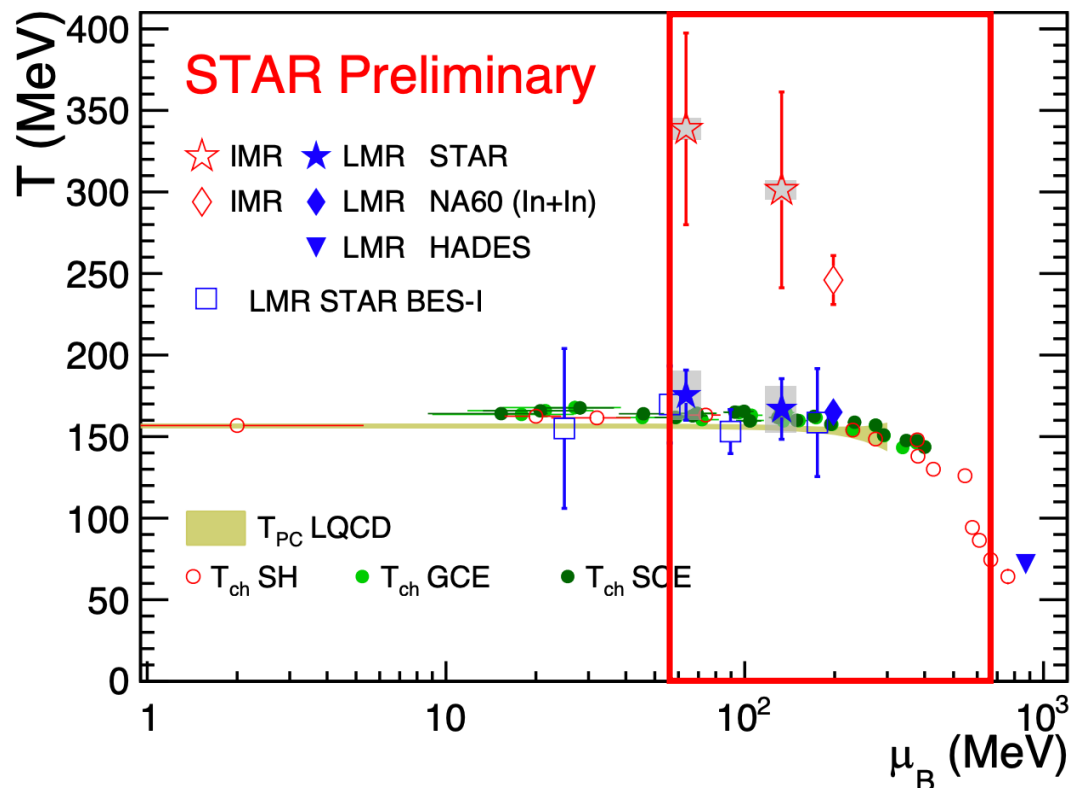
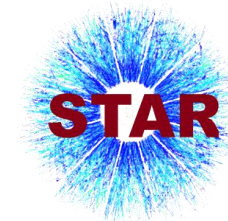


T in 27 and 54.4 GeV are consistent with each other

$T > T_{pc}$  (156 MeV): emission dominantly from QGP



# Phase diagram mapping with dielectrons



$T_{LMR}$  close to  $T_{ch}$  and  $T_{pc}$   
 $\rho$  meson dominantly emitted around phase transition

$T_{IMR}$  higher than  $T_{LMR}$ ,  $T_{ch}$  and  $T_{pc}$   
dielectron dominantly emitted from QGP phase

High statistics data sample between 7.7 GeV and 19.6 GeV in STAR BES-II will help map the kink region

Enhanced tracking and particle identification capabilities with iTPC and eTOF upgrades

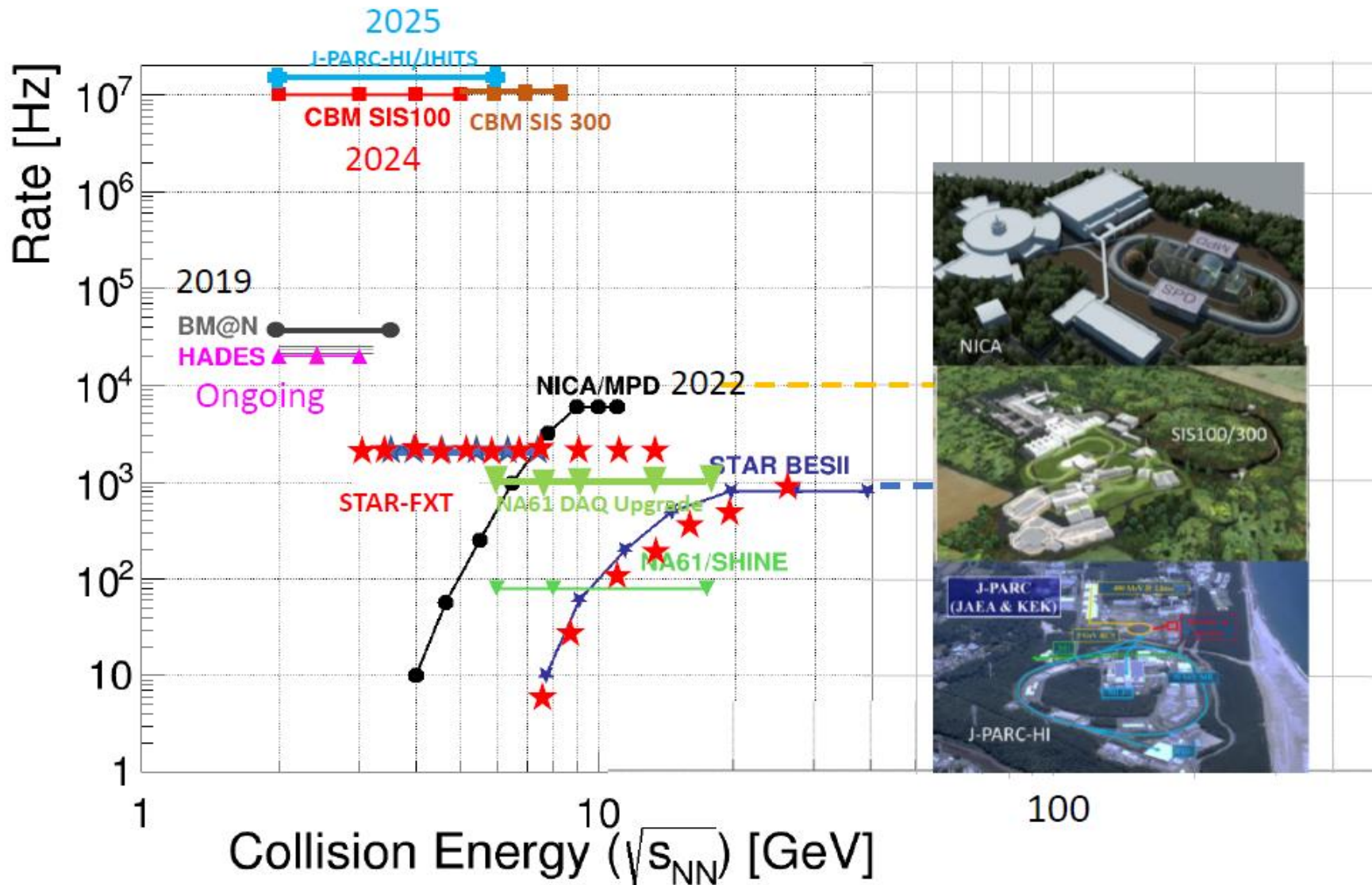
NA60: EPJC (2009) 59 607–623

HADES: Nature Physics 15, 1040-1045 (2019)

$T_{ch}$  SH: P. Braun-Munzinger et al. Nature 561, 321-330 (2018)

$T_{ch}$  GCE/SCE: STAR PRC **96**, 044904 (2017)

# HIC facilities and experiments



SPS up to 160 GeV

NICA/MPD is a Collider exp.  
NICA single beam of about 10 GeV

Nuclotron reaches up to 3.5 GeV

JPARC up to about 18 GeV

# Summary

---



- ✓ BES-I was performed between 2010 – 2014 and demonstrated the capability of RHIC to operate at low energies
- ✓ BES-II has increased statistics by a factor of 10 for most of the energies and provided additional data with FXT mode of STAR detector
- ✓ BES-II data were taken after several detector upgrades
- ✓ Previous energy scans had demonstrated that at low energies many signatures of sQGP are turned off
- ✓ The first results are from the lowest energy FXT system and these demonstrate that the system is clearly in the hadronic gas phase (as expected)
- ✓ Data taking has been very successfully completed and new results are on the way



---

Thank you for the attention!

Part of this work has been supported by Russian Science Foundation under grant № 22-72-10028



# Backup slides



$\sqrt{s_{NN}}$ (GeV)	Events ( $10^6$ )	Year	$\mu_B$ (MeV)	$T_{CH}$ (MeV)
200	350	2010	25	166
62.4	67	2010	73	165
54.4	1200	2017	90	
39	39	2010	112	164
27	70	2011	156	162
19.6	36	2011	206	160
14.5	20	2014	264	156
11.5	12	2010	315	152
9.2	0.3	2008	355	140
7.7	4	2010	420	140

# BES-II statistics and run time



Recent BES-II, FXT and 200 GeV datasets (years 2018-2021)



BES-I (years 2010, 2011, 2014)

$\sqrt{s_{NN}}$ (GeV)	No. of events (million)
7.7	4
11.5	8
19.6	17.3
27	33
39	111

$\sqrt{s_{NN}}$ (GeV)	Beam Energy (GeV/nucleon)	Collider or Fixed Target	$y_{\text{center of mass}}$	$\mu^B$ (MeV)	Run Time (days)	No. Events Collected (Request)	Date Collected
200	100	C	0	25	2.0	138 M (140 M)	Run-19
27	13.5	C	0	156	24	555 M (700 M)	Run-18
19.6	9.8	C	0	206	36	582 M (400 M)	Run-19
17.3	8.65	C	0	230	14	256 M (250 M)	Run-21
14.6	7.3	C	0	262	60	324 M (310 M)	Run-19
13.7	100	FXT	2.69	276	0.5	52 M (50 M)	Run-21
11.5	5.75	C	0	316	54	235 M (230 M)	Run-20
11.5	70	FXT	2.51	316	0.5	50 M (50 M)	Run-21
9.2	4.59	C	0	372	102	162 M (160 M)	Run-20+20b
9.2	44.5	FXT	2.28	372	0.5	50 M (50 M)	Run-21
7.7	3.85	C	0	420	90	100 M (100 M)	Run-21
7.7	31.2	FXT	2.10	420	0.5+1.0+scattered	50 M + 112 M + 100 M (100 M)	Run-19+20+21
7.2	26.5	FXT	2.02	443	2+Parasitic with CEC	155 M + 317 M	Run-18+20
6.2	19.5	FXT	1.87	487	1.4	118 M (100 M)	Run-20
5.2	13.5	FXT	1.68	541	1.0	103 M (100 M)	Run-20
4.5	9.8	FXT	1.52	589	0.9	108 M (100 M)	Run-20
3.9	7.3	FXT	1.37	633	1.1	117 M (100 M)	Run-20
3.5	5.75	FXT	1.25	666	0.9	116 M (100 M)	Run-20
3.2	4.59	FXT	1.13	699	2.0	200 M (200 M)	Run-19
3.0	3.85	FXT	1.05	721	4.6	259 M -> 2B(100 M -> 2B)	Run-18+21

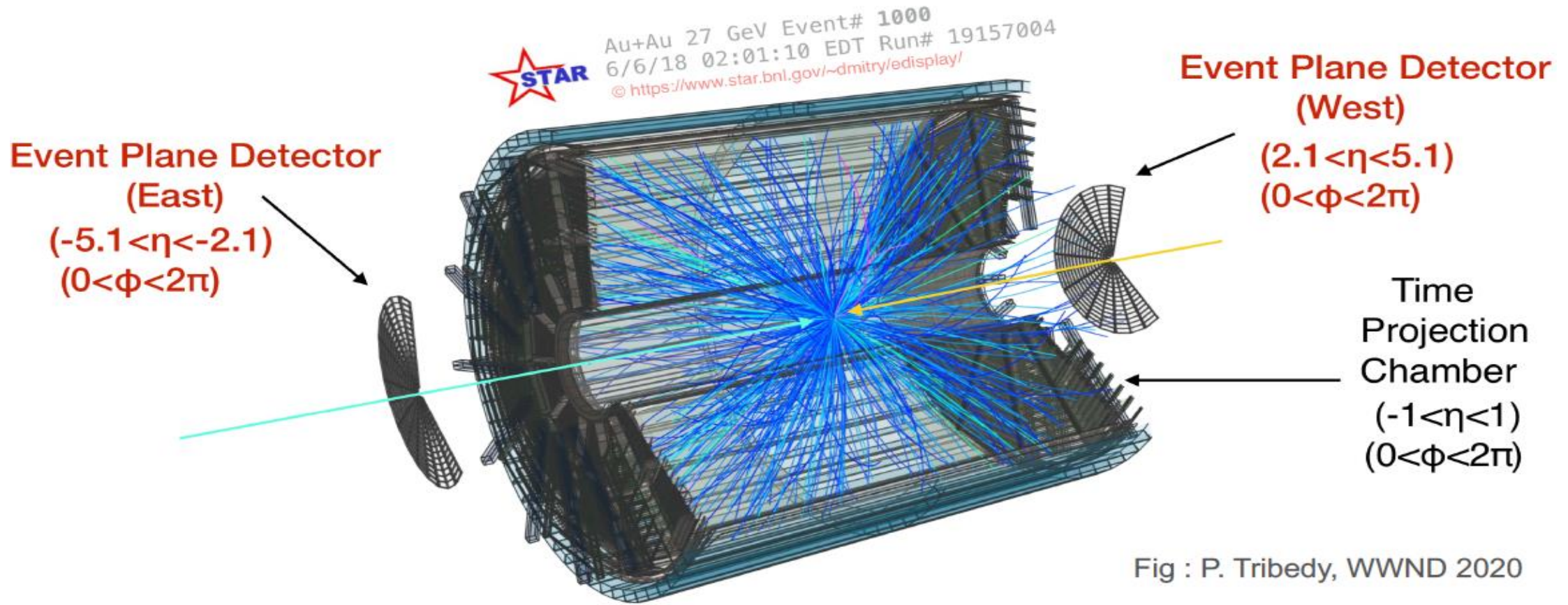


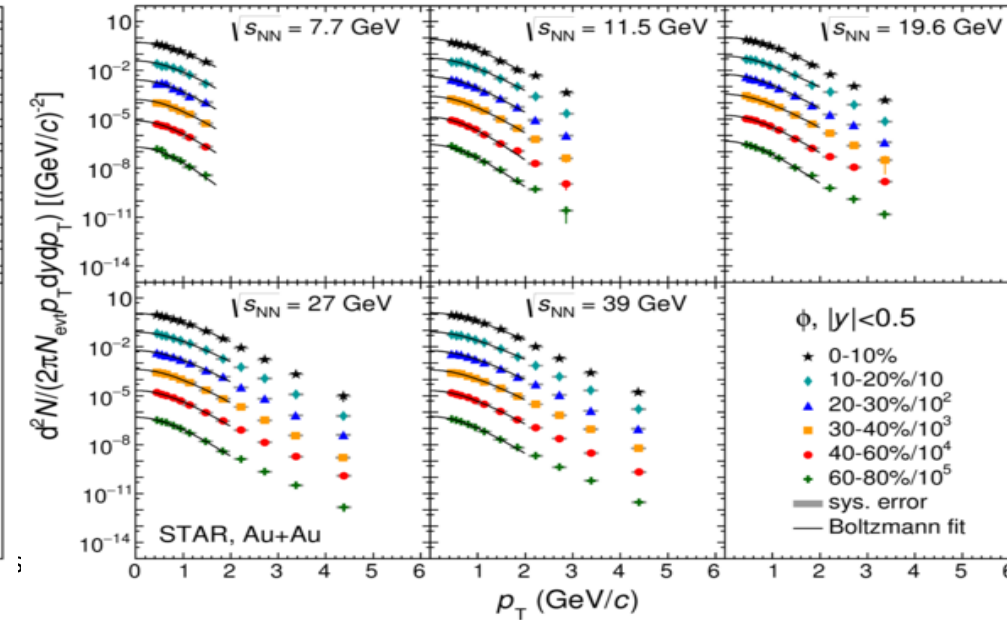
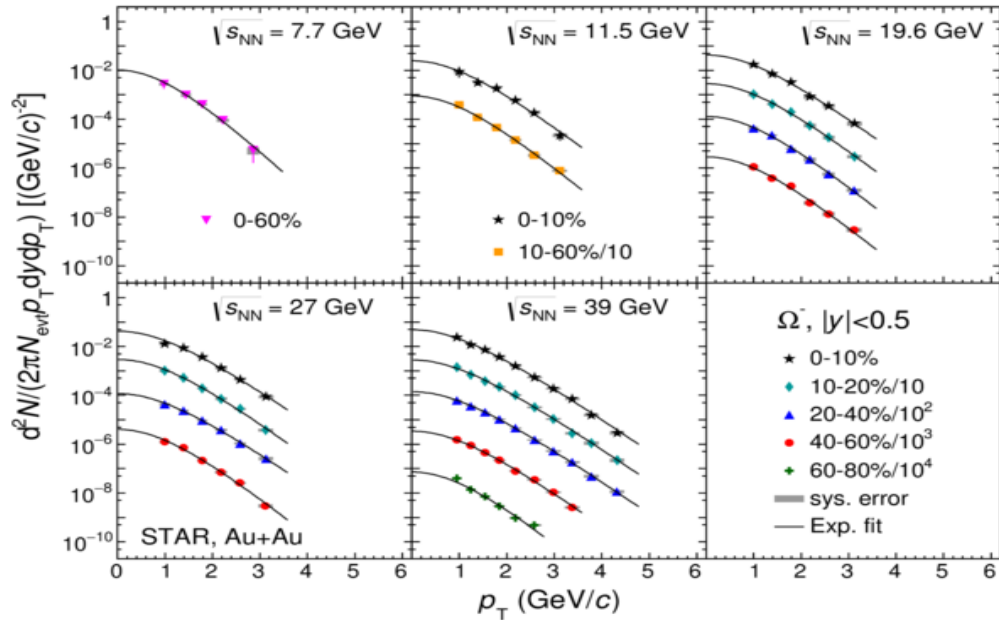
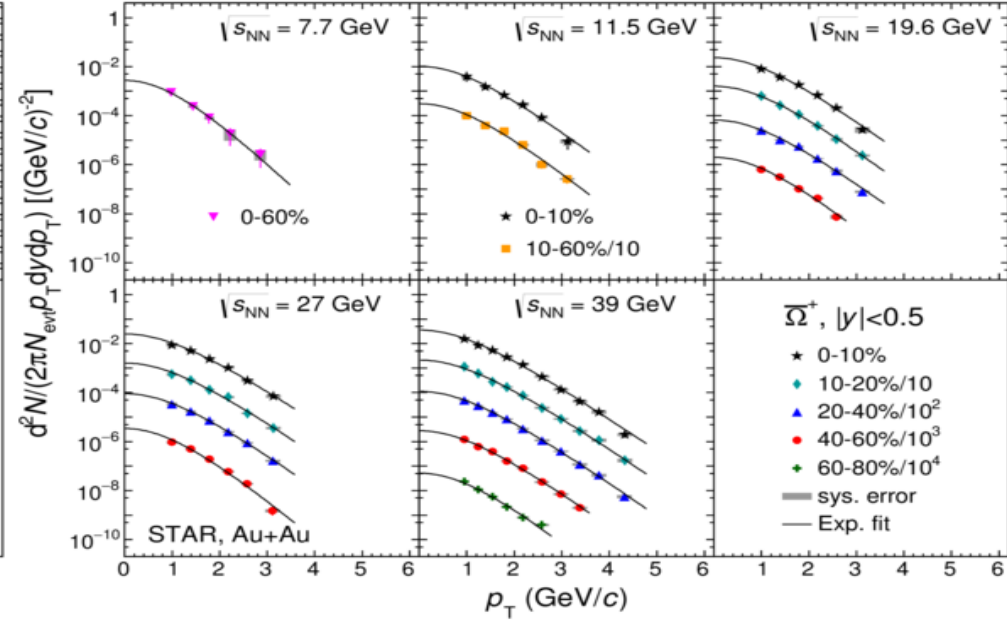
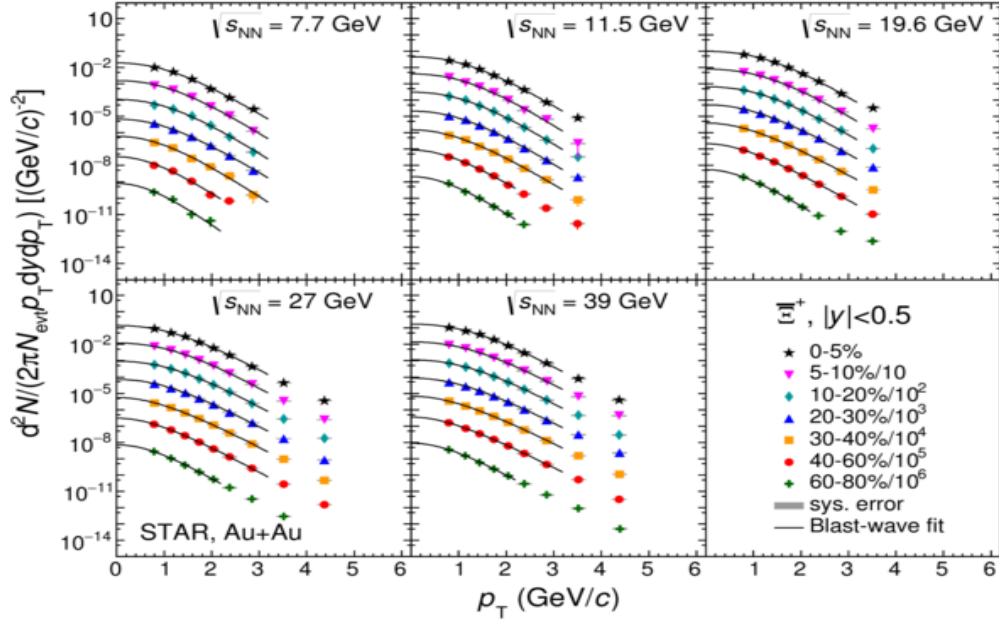
Fig : P. Tribedy, WWND 2020

Full azimuthal coverage  
Large separation in  $\eta$  between TPC and EPD

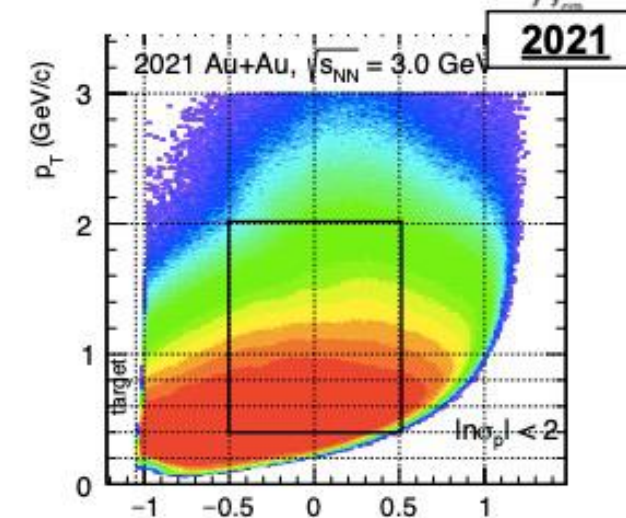
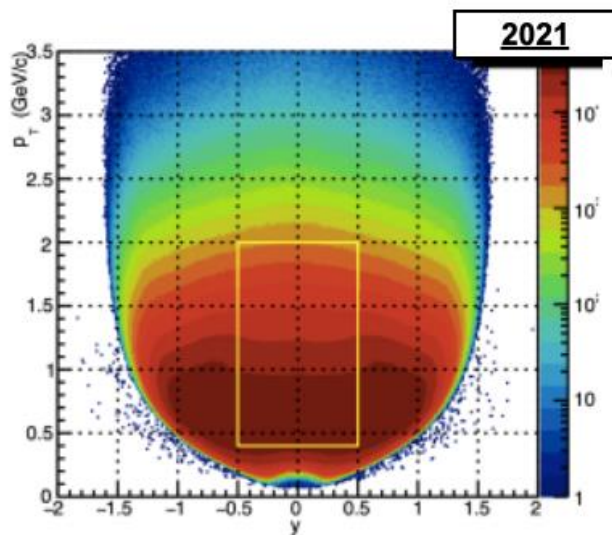
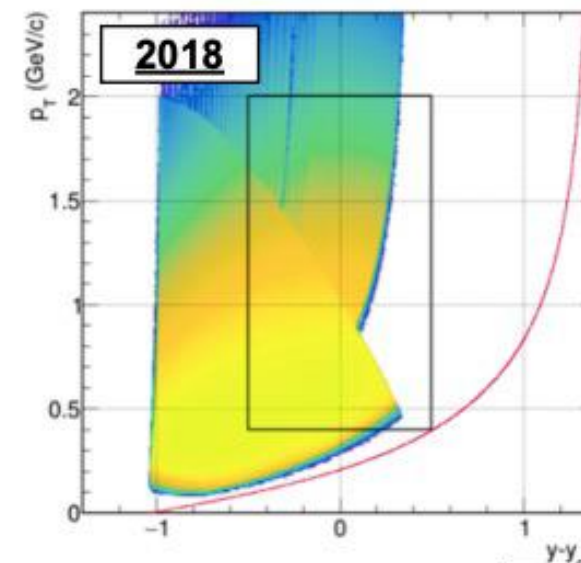
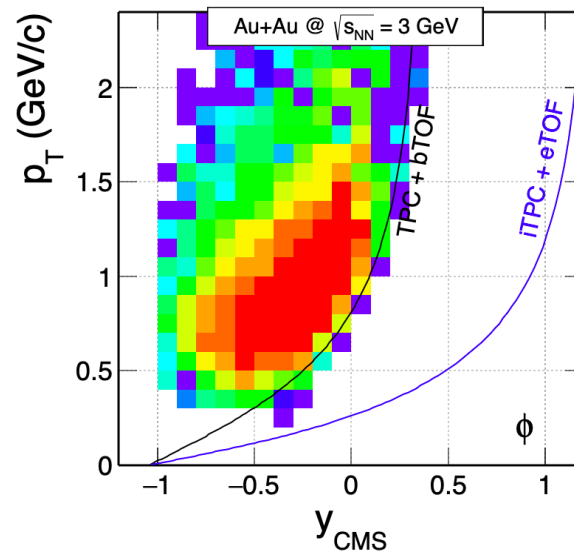
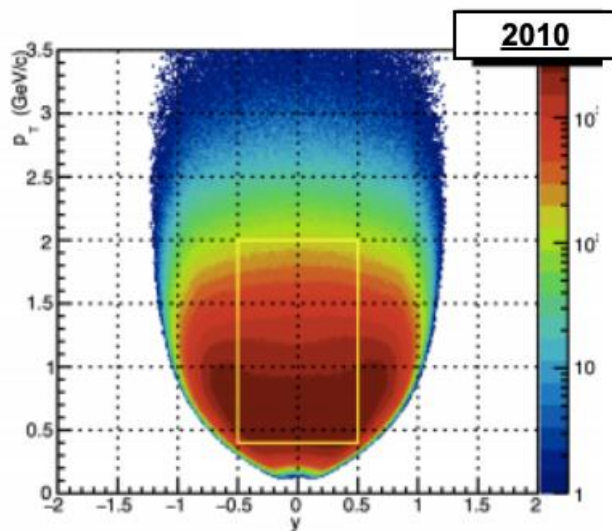
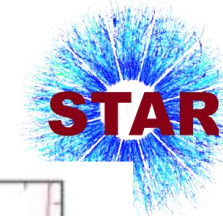
J. Adams et al. Nucl. Instrum. Meth. A 968 (2020)



# Strange particle production at BES-I



# New acceptance



# Light nuclei acceptance

